Transp Porous Med (2010) 82:215–246
DOI 10.1007/s11242-009-9509-8

Evaluation of Potential Changes in Groundwater Quality in Response to CO_2 Leakage from Deep Geologic Storage

J. A. Apps · L. Zheng · Y. Zhang · T. Xu · J. T. Birkholzer

Received: 15 January 2009 / Accepted: 18 November 2009 / Published online: 16 January 2010

Abstract Concern has been expressed that carbon dioxide (CO_2) leaking from deep geological storage could adversely impact water quality in overlying potable aquifers by mobilizing hazardous trace elements. In this article, we present a systematic evaluation of the possible water quality changes in response to CO_2 intrusion into aquifers currently used as sources of potable water in the United States. The evaluation was done in three parts. First, we developed a comprehensive geochemical model of aquifers throughout the United States, evaluating the initial aqueous abundances, distributions, and modes of occurrence of selected hazardous trace elements in a large number of potable groundwater quality analyses from the National Water Information System (NWIS) database. For each analysis, we calculated the saturation indices (SIs) of several minerals containing these trace elements. The minerals were initially selected through literature surveys to establish whether field evidence supported their postulated presence in potable water aquifers. Mineral assemblages meeting the criterion of thermodynamic saturation were assumed to control the aqueous concentrations of the hazardous elements at initial system state as well as at elevated CO_2 concentrations caused by the ingress of leaking CO_2. In the second step, to determine those hazardous trace elements of greatest concern in the case of CO_2 leakage, we conducted thermodynamic calculations to predict the impact of increasing CO_2 partial pressures on the solubilities of the identified trace element mineral hosts. Under reducing conditions characteristic of many groundwaters, the trace elements of greatest concern are arsenic (As) and lead (Pb). In the final step, a series of reactive-transport simulations was performed to investigate the chemical evolution of aqueous As and Pb after the intrusion of CO_2 from a storage reservoir into a shallow confined groundwater resource. Results from the reactive-transport model suggest that a significant increase of aqueous As and Pb concentrations may occur in response to CO_2 intrusion, but that the maximum concentration values remain below or close to specified maximum contaminant levels (MCLs). Adsorption/desorption from mineral surfaces may strongly impact the mobilization of As and Pb.

J. A. Apps · L. Zheng · Y. Zhang · T. Xu · J. T. Birkholzer (✉)
Earth Sciences Division, Lawrence Berkeley National Laboratory, 1 Cyclotron Road,
MS 90-1116, Berkeley, CA 94720, USA
e-mail: jtbirkholzer@lbl.gov

Keywords CO_2 leakage · Groundwater contamination · Hazardous trace elements

1 Introduction and Approach

Carbon dioxide (CO_2) buildup in the atmosphere can be mitigated through its capture from stationary sources such as coal-burning power plants and subsequent injection into suitable deep geologic formations for long-term storage. Proper site selection and management of CO_2 storage projects will ensure that the risks to human health and the environment are low (Bachu 2000). However, it is possible that CO_2 could migrate from a storage formation into overlying aquifers containing drinking water. The schematic in Fig. 1 shows such a scenario, where a local high-permeability pathway—such as a permeable fault or an open abandoned well—would allow buoyant supercritical CO_2 to escape from depth and reach a shallow aquifer. The CO_2 would typically reach shallow aquifers after transformation to a gaseous state and partially or completely dissolve into the groundwater.

Dissolution of CO_2 in a freshwater aquifer increases the total concentration of dissolved carbonate and thus increases acidity. The increased acidity can enhance the dissolution of minerals, including those containing hazardous trace elements. The resulting increase in concentration of hazardous trace elements could detrimentally impact groundwater quality, to the extent that the Maximum Contaminant Levels (MCLs) mandated by U.S. Environmental Protection Agency (EPA; U.S. Environmental Protection Agency 2004) as part of their national drinking standards are exceeded. Decreasing pH can also enhance desorption of hazardous trace elements from adsorption sites on host rock mineral surfaces, particularly from clays, iron oxyhydoxides, carbonates, and coatings on detrital minerals (Kharaka et al. 2006), and may also release them from ion exchange sites in the inter-layer positions in clays.

The potential mobilization of hazardous trace elements in response to CO_2 intrusion has not been systematically studied until now. Wang and Jaffe (2004) conducted reactive-transport simulations considering the migration of CO_2 into aquifers with a significant volume

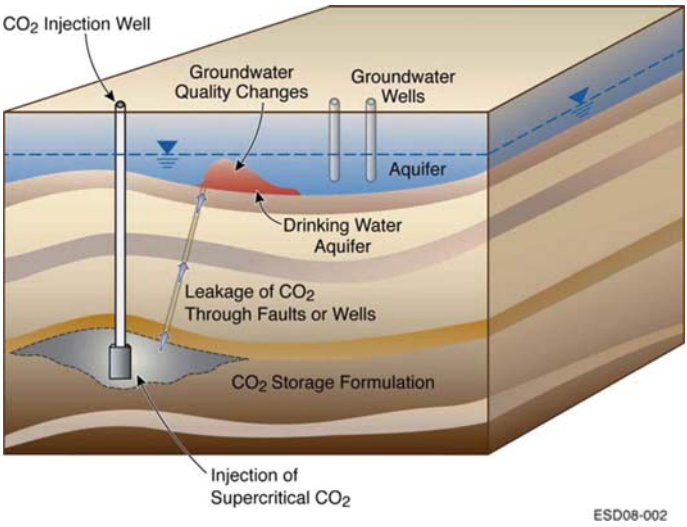

Fig. 1 Schematic illustration of potential groundwater quality changes in response to CO_2 leakage from deep storage sites

fraction of a lead sulfide, galena (PbS), comprising the aquifer rocks. Their results suggest that enhanced dissolution of galena would cause the MCL for lead to be exceeded in aquifers where the pH is poorly buffered by the host rock minerals. It should be noted, however, that the authors intended only to illustrate the potential effects of CO_2 intrusion on water quality, as their study involves greatly simplified host rock mineral compositions. Thus, while their results highlight a potential concern, it is not clear how severe and widespread the problem would be in reality. Carroll et al. (2008) evaluated the impact of CO_2 intrusion into the High Plains Aquifer in the United States using a reactive-transport simulator. The purpose of their study was to understand the resulting pH changes and to evaluate the detectability of the acidic plume in the aquifer; the issue of mobilization of hazardous trace elements was not addressed.

Zheng et al. (2009) recently reported on a field experiment with CO_2 injection into a shallow aquifer in Montana. Preliminary groundwater analyses suggest that the dissolution of CO_2 leads to the mobilization of trace metals. Smyth et al. (2008) observed a pH decrease and increased cation concentrations in laboratory batch experiments with diverse aquifer rocks exposed to CO_2-charged water. McGrath et al. (2007) evaluated the potential impact of carbon dioxide contained in municipal solid waste (MSW) landfill gas on the release of cadmium from uncontaminated native soils. Based on soil leaching experiments and geochemical modeling, the authors concluded that the observed increases in aqueous cadmium in the field were likely caused by the CO_2 dissolution into the groundwater and the related increase of acidity, causing mobilization of cadmium from naturally occurring otavite (or cadmium carbonate) in the soils.

It is obvious from the limited research conducted so far that the vulnerability of potable groundwater resources should be assessed in anticipation of large-scale capture and deep underground storage of CO_2. The current article addresses one aspect of this issue, describing a generic evaluation of possible water quality changes in response to CO_2 intrusion into potable aquifers in the United States. Such waters contain total dissolved solids concentrations far less that the maximum 10,000 mg/l permitted in an Underground Source of Drinking Water (USDW), as defined by the EPA. Because the study is generic, it should be understood that additional geochemical modeling and simulation analysis will be necessary to address site-specific conditions, ideally supported by laboratory and field experiments. It should be noted further that the geochemical modeling studies reported in this article assume the transport and intrusion of pure CO_2. Leaking CO_2 may carry organic compounds leached at depth, or co-injected trace contaminants, such as H_2S. The potential ramifications of impure CO_2 transport and consequent contamination of potable aquifers be transported contaminants will be explored in future studies.

The goal of our study is to understand, for a range of relevant aquifer conditions, the potential for the mobilization of selected hazardous trace elements by the ingress of CO_2, how these elements might be redistributed, both spatially and temporally, and whether MCLs would be exceeded. A reactive-transport model was developed to simulate multiphase flow of CO_2 and water, and to predict the fate and migration of selected hazardous trace elements in the groundwater (Sect. 4). Prior to this modeling effort, a preliminary assessment of CO_2-related water quality changes was conducted by calculating the expected equilibrium concentrations of hazardous elements as a function of the partial pressure of CO_2 in groundwater with a representative composition (see Sect. 3).

As in any numerical simulation study, reliable model predictions can only be achieved when model conditions and parameters, such as the initial water chemistry, oxidation state, and initial abundance and distribution of selected hazardous trace elements, are both realistic and representative, and when all relevant processes are taken into account. In order to

ensure that these requirements are adequately represented, a comprehensive review of the geochemical literature was conducted in conjunction with a thermodynamic evaluation of a large number of potable groundwater analyses from aquifers throughout the United States, which were retrieved from the NWIS database (see Sect. 2). An important step in this evaluation was the identification of mineral hosts that partially or completely control the aqueous concentrations of hazardous trace elements in potable groundwaters. The mineral hosts are identified as those containing a hazardous element either as an essential component, or as a non-essential component substituting for an essential component in solid solution. With one exception, regarding the behavior of antimony, those hosts meeting the criterion of thermodynamic saturation were assumed also to control the aqueous concentrations of hazardous elements after the ingress of CO_2, as evaluated in the equilibrium calculations in Sect. 3 and in the reactive-transport simulations in Sect. 4.

In this article, we can only briefly discuss the full scope of the comprehensive geochemical evaluations and predictions conducted in this study. Considerably more details are provided in a report by Birkholzer et al. (2008).

2 Geochemical Model Definition

The comprehensive geochemical model developed in this section provides the necessary input for the equilibrium and reactive-transport models applied in Sects. 3 and 4. The steps taken in developing the geochemical model included: (1) examination of a large number of potable groundwater quality analyses (about 38,000) from potable water aquifers throughout the United States to determine concentration distributions of selected trace elements, (2) identification of potential trace element mineral hosts through literature reviews of such areas as epithermal ore deposition, coal mineralogy, and the authigenesis of contemporaneous sediments, (3) acquisition of thermodynamic data for the host minerals of interest as well as thermodynamic data on aqueous species and complexes of the trace elements, especially sulfide and selenide complexes of Cd, Hg, Pb, and Zn, and (4) geochemical evaluation of all groundwater quality analyses to identify which minerals hosting hazardous elements might saturate the groundwater. Each of these steps is discussed in detail as follows.

From the complete list of EPA-identified hazardous inorganic chemicals (U.S. Environmental Protection Agency 2004), we selected the following elements for inclusion in the geochemical model: arsenic (As), barium (Ba), cadmium (Cd), mercury (Hg), lead (Pb), antimony (Sb), selenium (Se), and uranium (U). The selection was based, in part, on the potential likelihood of MCLs being exceeded, e.g., Pb (Wang and Jaffe 2004), as well as As and U (Focazio et al. 2006), on their very low MCLs, e.g., Cd, Hg, and Sb, and on their good detectability in groundwaters, e.g., As, Ba, and U. Although, not considered hazardous, we also included zinc (Zn), due to the common association of Cd with Zn in sphalerite (ZnS). Other metals known to be solubilized by CO_2 intrusion, e.g., Fe and Mn (Kharaka et al. 2006) were not included, because they are not deemed to be particularly hazardous (U.S. Environmental Protection Agency 2004).

Some interesting challenges arise with the development of a geochemical model describing the thermodynamic response of the selected trace elements to changing partial pressure of CO_2 in potable aquifers. First, the chemical behavior of these elements differs considerably depending on whether the aquifer is in a reduced or oxidized state, but it is not easy to establish the oxidation state from standard water quality analyses. Second, the mode of occurrence for each element, regardless of oxidation state, varies, depending on aquifer mineralogy, and the natural abundance of each element. Although several of the selected elements form

discrete minerals where the element is an essential component under reducing conditions, such as Pb in galena, others substitute for a more abundant element in solid solution, as occurs with Cd substitution for Zn in sphalerite (ZnS). However, at the temperatures prevailing in potable aquifers, the extent of solid solution is limited and excess Cd could be taken up by cadmoselite (CdSe), while co-existing in thermodynamic equilibrium with sphalerite. Due to these complexities, it is not initially clear whether some of the selected trace elements are present in solid solution or as discrete minerals. Under oxidizing conditions, the solubilities of all of the trace elements except Ba are much higher, and in the case of As, it is likely that no mineral host containing arsenic as an essential component may exercise thermodynamic control before its MCL is exceeded.

The natural abundances of the selected trace elements in aquifer host rocks are so low that detection and identification of those discrete mineral hosts containing a hazardous trace element as an essential component is almost impossible using conventional petrologic analyses. Thermodynamic arguments indicate that the natural abundances of the selected elements in sedimentary rocks are sufficient for all, but Ba and U to be sequestered under reducing conditions primarily in trace concentrations of chalcogenide minerals, either as in essential components, or in solid solution, and where it is also assumed that the preponderance of each element is no longer sequestered in unaltered detrital minerals. Calculations suggest further that a minor fraction of each element, depending on its chemistry, might also be distributed over adsorption and ion exchange sites associated with framework and matrix minerals comprising the aquifer host rock. For the most part, the presence of trace concentrations of these postulated mineral hosts can be inferred only through an evaluation of the behavior of trace element concentrations in the potable groundwaters under an assumed equilibrium state. Caution must be exercised in adopting this assumption, as it is well-known that detrital minerals, e.g., feldspars, and organic matter present in aquifer rocks may be subject to diagenesis over periods up to millions of years, and rarely achieve thermodynamic equilibrium. Furthermore, many shallow groundwaters are out of equilibrium with respect to redox reactions (Lindberg and Runnels 1984; Stefansson et al. 2005; Washington et al. 2004). The role that a potential disequilibrium state plays with respect to redox potential is discussed further in Appendix B.

2.1 Concentrations of Hazardous Trace Elements in Potable Groundwaters

The 38,000 groundwater quality analyses drawn from wells in the United States were downloaded from the National Water Information System (NWIS) database. The criteria for selection of the waters were that they had to be recovered from underground sources for drinking water purposes, that each sample had to be analyzed for at least one of the selected trace elements, and that the analyses had to be complete for all major cations and anions and pH. Such a selection procedure does not necessarily result in a cohort that is representative of all potable groundwaters in the Unites States. The water quality analyses may be biased toward those taken from a large number of small shallow wells serving isolated farmsteads, rather than the smaller number of large production volume wells tapping deep confined aquifers, and serving municipal water supplies. Furthermore, the density of farmsteads is related, in part, to the distribution of arable land or cropland, and is sparser where rangeland predominates as is more typical in the Southwest, which could bias the sample toward groundwaters that are anoxic or reducing. A bias may also have been introduced, because hazardous trace elements are more likely to be analyzed whenever a potential problem might be suspected. These potential, yet unquantified biases could impact the findings of the study, as is discussed in a later section. Nevertheless, any such biases, if real, would lead to findings that are inherently conservative, which are favored from the regulatory perspective.

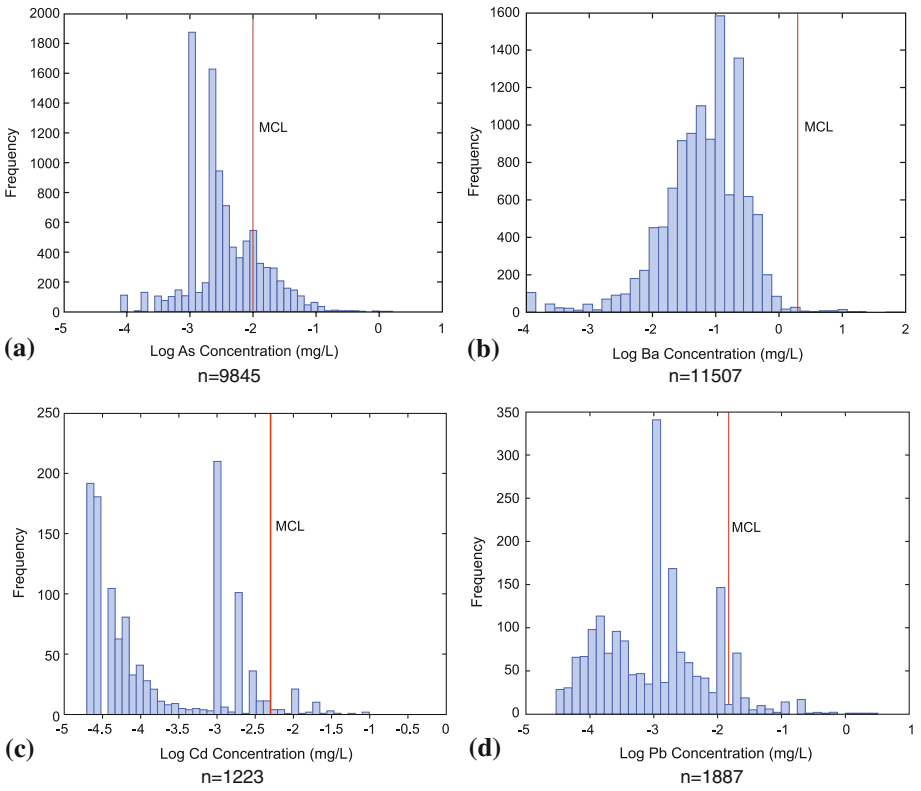

Fig. 2 Histograms showing the concentration distributions of selected hazardous elements in more than 38,000 analyses of potable groundwaters in the United States. MCL signifies the maximum contaminant level for each constituent. *n* indicates the number of data points used for histogram

The population of analyses for each trace element was divided into uniform bins, representing incremental concentration ranges on a logarithmic scale, and plotted as histograms. Selected histograms for As, Ba, Cd, and Pb are given in Fig. 2a–d. For comparison, the MCL is also plotted. With the exception of a few outliers, most of the elements meet MCL requirements for the majority of groundwater samples in the database. A significant minor percentage of groundwaters containing As and U (not shown in Fig. 2) exceeds the MCL for those elements, however, as also noted by Focazio et al. (2006).

The histograms shown in Fig. 2 were plotted without regard to analytical method or accuracy. All histograms are characterized by isolated bins with anomalously high populations. These bins contain analyses with "round number" concentrations, such as 0.001 or 0.002 mg/l, considered to be stemming from analytical artifacts. (The NWIS database has been compiled over a number of years, during which time newer, more accurate analytical methods have supplanted earlier methods.) In some histograms, notably those for Cd and Pb, bimodal distributions are evident, due primarily to the results of insufficiently sensitive analytical methods reporting positive value artifacts. Such artifacts, and the possible tendency to analyze samples with known or suspected contamination, could skew the data sets toward higher values. Therefore, only data obtained using the most sensitive methods are considered in subsequent evaluations in this article. However, with respect to Cd and Hg,

the fraction of detectable values using even the most sensitive analytical methods is only 36 and 12%, respectively (Birkholzer et al. 2008), meaning that the majority of all samples have aqueous Cd and Hg concentrations too low to be detected, which would result in a bias when calculating model concentrations for these elements. The respective hypothetical modal values of concentration were, therefore, estimated on the assumption that the distributions observed for As, Ba, U, and Zn—where the most sensitive analytical methods are sufficient for more than 90% of all samples—are lognormal and that Cd and Hg would display comparable distributions had the analytical methods been sufficiently sensitive for these elements. The hypothetical modal log concentrations (mg/l) for Cd and Hg are estimated to be ≈ -4.7 and ≈ -5.0, respectively. This information is necessary for subsequent evaluations of thermodynamic controls affecting Cd and Hg behavior in potable groundwaters.

2.2 Identification of Potential Mineral Hosts Controlling the Concentration of Hazardous Elements

Very few information is available in the literature concerning the mode of occurrence of the selected trace metals in shallow aquifer host rocks. This is hardly surprising, given the exceedingly low natural abundances of the trace metals, and the technical challenges in isolating and characterizing their mineral hosts when present in micro-concentrations (Craig Cooper and Morse 1999). However, extensive studies have been undertaken over many years to characterize their distributions in the various mineral components of coals (e.g., Finkelman 1981; Kolker et al. 2002). Because many trace elements are environmentally hazardous, potential coal pretreatment processes to minimize their release to the atmosphere following combustion are of considerable interest. The detection of trace element mineral hosts in a coal matrix in polished sections by optical microscopy is somewhat easier than in a corresponding arenaceous host rock, and sequential leaching procedures facilitate their separation for analysis. Furthermore, the sustained reducing environment induced by organic matter in coal beds, and their duration of burial, allow sequestration and enrichment of trace elements in discrete mineral hosts. As a result, these hosts are more readily identified and characterized in coal than in arenaceous sedimentary rocks. It is of course obvious that coals differ markedly in composition from a typical shallow aquifer host rock. A typical arenaceous aquifer rarely contains more than 2 wt% of organic matter, in contrast to coal, which in some instances exceeds 95 wt%. Also, the "ash" content of exploitable coal rarely exceeds 30 wt%, whereas nearly 100 wt% of an aquifer host rock consists of inorganic material. Yet, these differences do not necessarily impact the identification of mineral hosts expected to occur in potable aquifers, as is discussed further in Appendix B.

The coal literature helps not only in the identification of mineral hosts where the trace element is an essential component using optical microscopy, but sequential selective leaching procedures also allow characterization of the trace element distributions between pyrite, "ash", and the organic phases. Further studies of the concentrations of the selected elements, notably As, Hg, Sb, and Se in pyrite, allow a qualitative, if not semi-quantitative measure of the extent of potential solid solution substitution of these elements in pyrite.

Elsewhere in the literature, studies have been made regarding the partitioning of trace elements in secondary sulfides and/or organic matter in recent sediments (Davies-Colley et al. 1985; Huerta-Diaz and Morse 1992; Benoit et al. 1999). In particular, Huerta-Diaz and Morse (1992) investigated the partitioning of trace elements into authigenic pyrite in marine sediments as a function of depth from the sediment/aqueous interface. Information from such studies supplements and sometimes corroborates information derived from the coal literature

Table 1 Potential mineral hosts for hazardous trace elements under reducing conditions

Hazardous trace elements	Potential mineral controls	
	Solid solution component	Discrete mineral
As	$(FeAsS)_{py}$	Arsenopyrite (FeAsS)
Ba	–	Barite ($BaSO_4$); Witherite ($BaCO_3$)
Cd	$(CdS)_{sph}$	Greenockite (CdS); Cadmoselite (CdSe)
Hg	$(HgS)_{py}$	Cinnabar (HgS); Tiemannite (HgSe)
Pb	–	Galena (PbS); Clausthalite (PbSe)
Sb	$(FeSbS)_{py}$	Stibnite (Sb_2S_3); Kermesite (Sb_2S_2O); Antimonselite (Sb_2Se_3); Gudmundite (FeSbS)
Se	$(FeSe_2)_{py}$	Ferroselite ($FeSe_2$); Dzharkenite ($FeSe_2$); Antimonselite (Sb_2Se_3); Cadmoselite (CdSe); Clausthalite (PbSe); Tiemannite (HgSe)
U	–	Uraninite (UO_2); Coffinite ($USiO_4$); Brannerite (UTi_2O_6)
Zn	–	Sphalerite (ZnS); Hemimorphite ($Zn_4Si_2O_7(OH)_2 \cdot H_2O$)

Note: py = pyrite, sp = sphalerite

despite the inherent limitations in identifying potential trace element mineral hosts other than the relatively abundant pyrite (Craig Cooper and Morse 1999). Heavy metal contamination from anthropogenic sources in harbor bottom muds and estuarine sediments also provides an opportunity to identify potential mineral hosts as is evident from the sparse literature on the subject (Luther et al. 1980; Lee and Kittirck 1984; Zaggia and Zonta 1997). Finally, the literature on low-temperature epithermal and sedimentary ore deposition provides valuable supporting information, especially in relation to phase relations between the chalcogenides. The extensive literature relating to uranium mineralization in association with organic matter in sedimentary host rocks also provides valuable insight regarding its potential mode of occurrence in potable water aquifers.

Table 1 summarizes the key findings of the literature review to identify plausible trace element mineral hosts expected in potable groundwaters. More details regarding the review are given in Birkholzer et al. (2008). These minerals are expected to occur under mainly reducing conditions, i.e., where the redox potential is most likely controlled by a pyrite/goethite or related buffer. Several other minerals likely to occur under more oxidizing conditions were also identified, but are not listed here for brevity. Solid solution substitution of the selected trace elements in silicates and carbonates was not pursued, although it is recognized that some fraction of the total concentrations of each trace element may be partitioned in these mineral classes which could impact their distribution in other mineral hosts.

2.3 Evaluation of Thermodynamic Controls with EQ3/6

We quantified the thermodynamic controls that may influence the concentration and distribution of the selected trace elements in the groundwater using the distribution-of-species code EQ3/6 (Wolery 1993). The 38,000 water quality analyses from the NWIS database were processed using automated procedures for selecting and entering species concentrations in the input file of EQ3/6 for each analysis in turn. Procedures were followed in selecting

preferred values of certain parameters wherever duplicate values were available, such as both field and laboratory measurements for pH. These procedures are described in greater detail in Birkholzer et al. (2008). The thermodynamic calculations were conducted for all plausible mineral hosts identified in Table 1, as well as some other minerals relevant to the integrity of the water samples. In order to determine whether certain minerals might be saturated, the saturation state of each mineral must be calculated. The saturation state is related to the Gibbs free energy (ΔG_r) associated with the dissolution of the mineral, thus

$$\Delta G_r = RT \ln\left(\frac{IAP}{K}\right), \tag{1}$$

where R is the gas constant, T is the absolute temperature, IAP is the ion activity product of the dissolution reaction, and K is the corresponding equilibrium constant. The saturation state Ω is given by:

$$\Omega = \left(\frac{IAP}{K}\right), \tag{2}$$

and we follow the usual convention of defining the saturation index, SI, as $\mathrm{SI} = \log \Omega$.

EQ3/6 automatically calculates the SIs of relevant host rock minerals and trace element mineral hosts, and other parameters of interest such as charge imbalance, Eh, log $P(CO_2)$, and log $P(H_2S)$ as well as the distribution of aqueous complexes in solution for each water quality analysis. The database used by the code is a compilation of mineral solubility products and aqueous species dissociation constants. It was extensively revised and augmented to meet the needs of the study, as discussed further in Appendix A.

2.3.1 Integrity of Water Quality Analyses and Other Considerations

Preliminary runs conducted with EQ3/6 revealed certain aspects of the 38,000 sample data set that forced acceptance of compromises in evaluating thermodynamic controls. Among these issues are the temperature distribution in the groundwaters as shown in Fig. 3a, which shows a positive skew with a modal temperature at approximately 12°C. Most of the measured temperatures are lower than the standard 25°C at which many dissolution constants for aqueous complexes of the trace elements under study have been determined. Ideally, all EQ3/6 species

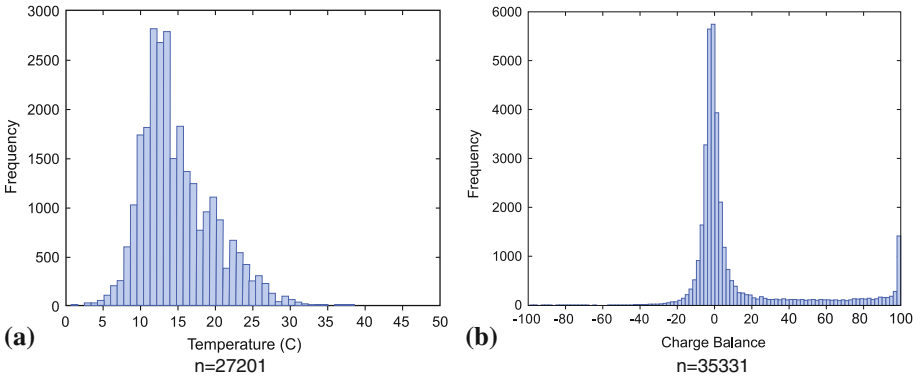

Fig. 3 Histogram showing (**a**) the temperature (°C) distribution and (**b**) the distribution of percentage charge imbalance of groundwater analyses from the NWIS database. *n* indicates the number of data points used for histogram

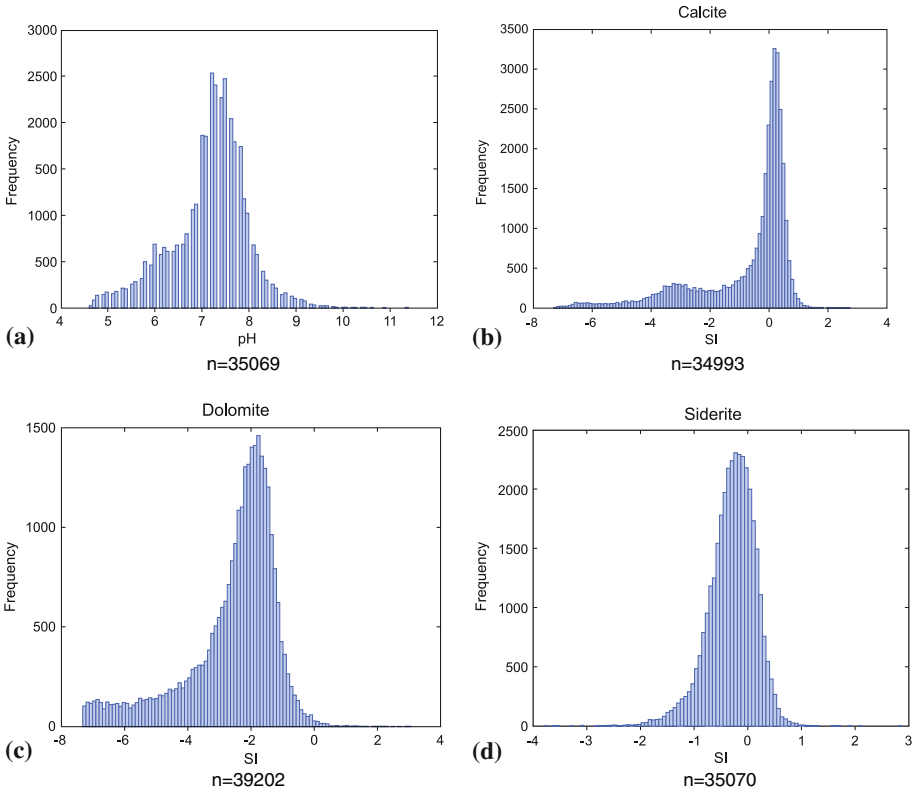

Fig. 4 Histogram showing (**a**) the pH distribution, (**b**) the calculated distribution of SIs for calcite, (**c**) dolomite, and (**d**) siderite, calculated using a subset of groundwaters from the NWIS database. No correction is made for charge imbalance. SI for siderite is calculated assuming saturation with respect to pyrite and goethite. *n* indicates the number of data points used for histogram

distributions should be computed at the ambient temperature of the groundwater. However, calculation of temperature dependence of these constants is difficult, especially with respect to critical oligomeric neutral sulfide and selenide complexes. Therefore, we decided to conduct all species distributions at 25°C, but subsequently take into account any biases in the computation of the overall uncertainty of the geochemical model. As shown in Fig. 3b, the mean charge imbalance of most analyses fell within the acceptable ±5% range.

Preliminary EQ3/6 runs also revealed other characteristics of the NWIS groundwaters relevant for further geochemical modeling, as illustrated in Fig. 4. The pH distribution in Fig. 4a indicates a modal value of about 7.6, but is skewed toward lower values. Most groundwaters appear to be saturated with respect to calcite (Fig. 4b), where the modal SI value is slightly above zero. Many dolomitic limestones are sources of drinking water in the eastern United States, and it is therefore of interest to examine the saturation state of all groundwaters with respect to dolomite. Figure 4c shows that dolomite is significantly undersaturated, with a modal SI value close to −1.8, which is consistent with reported occurrences of dedolomitization in shallow groundwaters (e.g., Edmunds et al. 1982; Plummer et al. 1990; Aravena et al. 1995; Hopkins and Putnam 2000). Figure 4d shows the calculated SI distribution for the

ferrous carbonate, siderite, where pyrite and goethite are assumed to control Eh, showing a modal value of about −0.2. Relaxing control of the redox state by coexisting goethite and pyrite would likely decrease the saturation state of siderite. The presence of this mineral in potable aquifers cannot be discounted, however, particularly when it is recognized that its stability increases with increasing $P(CO_2)$, and that it saturates if log $P(CO_2)$ exceeds −2 in the presence of pyrite.

It is worth mentioning that the $P(CO_2)$ in the NWIS groundwaters are on average about 1.5 orders of magnitude higher than atmospheric levels ($\text{Log}\, P(CO_2) = -3.5$), clearly indicating the potential of these groundwaters to degas CO_2 if exposed to air. The elevated $P(CO_2)$ in the subsurface environment is commonly attributed to the effects of microbial oxidation of organic matter. Indeed, this is most probably the case in shallow unconsolidated sediments undergoing active authigenesis. However, elevated $P(CO_2)$ can also result from thermogenesis of organic matter and decarboxylation, or from deeper diagenetic processes such as the translocation of CO_2 to shallower environments through diffusion/and or advective transport. Test calculations with EQ3/6 of groundwater saturated with respect to representative diagenetic mineral assemblages—including pyrite, goethite, calcite, and siderite—yield $P(CO_2)$ levels comparable to those observed without recourse to the external introduction of biogenic CO_2. Therefore, it remains an open question whether biogenic CO_2 modifies the diagenetic mineral assemblage, or whether the diagenetic assemblage specifies a partial pressure of CO_2 that is elevated with respect to that of the atmosphere.

In our evaluation of groundwaters, we assumed that the redox state was determined by the coexistence of goethite with pyrite at any given pH. In Appendix B, we discuss the reasons for making this assumption, and provide supporting independent evidence from the literature.

2.3.2 Saturation Indices of Trace Element Mineral Hosts in Potable Groundwaters

Figure 5 illustrates selected results from the thermodynamic analyses of NWIS groundwaters in the form of SI histograms for the elements As, Ba, Cd, and Pb and their potential solubility-controlling mineral hosts. The SI histogram for arsenopyrite (FeAsS; Fig. 5a) shows a modal value between −3.0 and −3.5, consistent with field observations indicating that As activity is controlled primarily by arsenopyrite in solid solution in pyrite (arsenian pyrite), e.g., see Reich and Becker (2006), at the relatively low As concentrations most commonly observed in the field. It should be noted, however, that very high As concentrations are sometimes observed under reducing conditions in groundwaters (Smedley and Kinniburgh 2002), suggesting possible saturation with respect to arsenopyrite. The SI histogram for barite ($BaSO_4$; Fig. 5b) shows a modal value close to zero, which suggests saturation with respect to this mineral. The corresponding histogram for witherite (not shown) gives a modal SI at −2, indicating that this mineral rarely, if ever, controls saturation of Ba in potable groundwaters.

The greenockite (CdS) histogram (Fig. 5c) displays a bi-modal distribution with SI maxima at about −3 and −0.5, which may be attributed, in part, to the bi-modal distribution of analyzed Cd concentrations (Fig. 2c). As stated before, most groundwaters contain Cd in concentrations undetectable by the most sensitive routine analytical methods. The actual modal value therefore is probably less than −3, suggesting a solid solution of CdS in sphalerite and/or galena. In contrast, the SI histogram for cadmoselite (CdSe) in Fig. 5d is relatively well-defined, with a modal value of about zero, suggesting that Cd^{+2} activity may be controlled by the presence of cadmoselite in some Cd-rich environments. SI histograms for galena (PbS) and clausthalite (PbSe; Fig. 5e, f) indicate that both are likely minerals controlling Pb in solution, which is consistent with the mode of occurrence of lead in coal (Finkelman 1981).

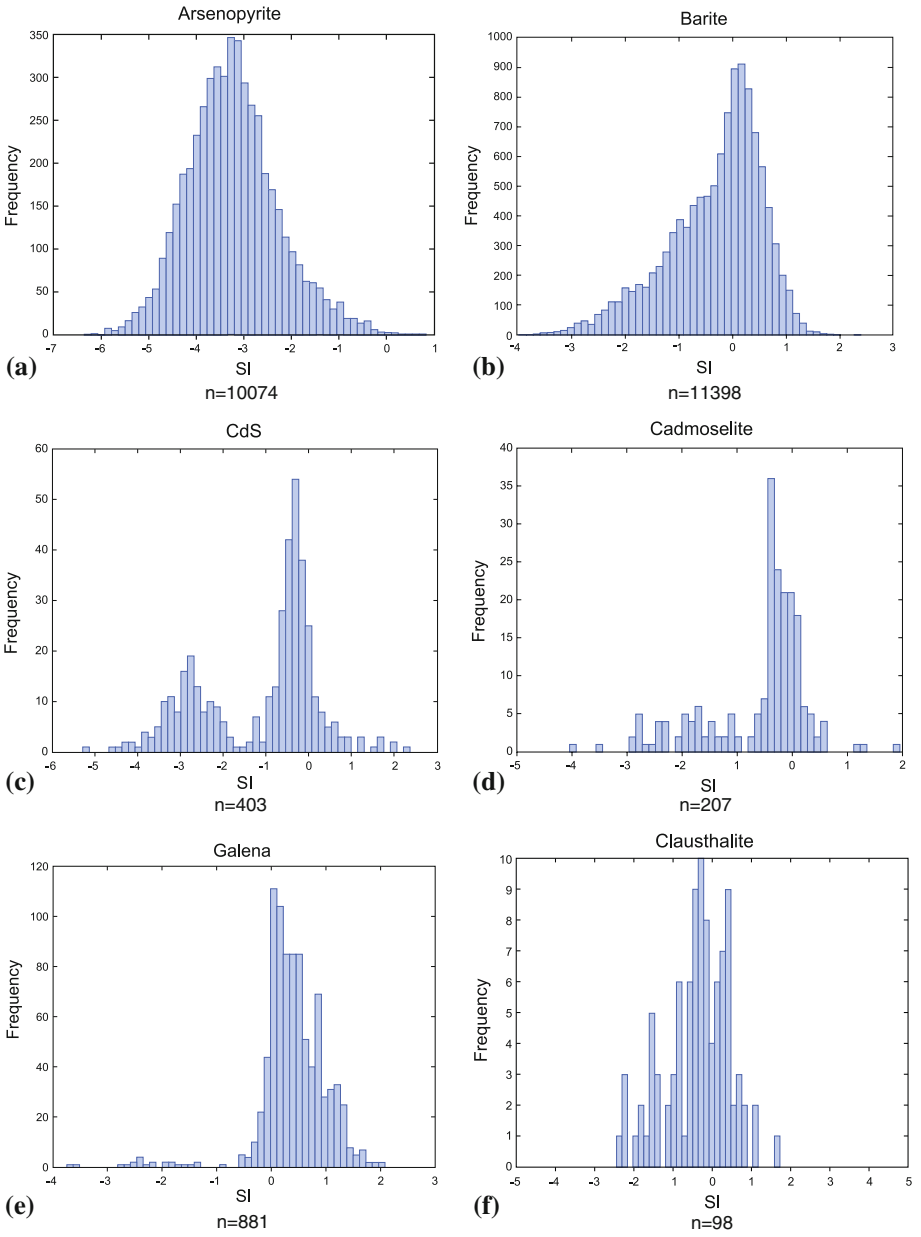

Fig. 5 SI histograms of selected mineral hosts: (**a**) Arsenopyrite, (**b**) Barite, (**c**) Greenockite, (**d**) Cadmoselite, (**e**) Galena, and (**f**) Clausthalite. SI values are calculated using a subset of groundwaters from the NWIS database, and assuming Eh to be defined by the coexistence of pyrite and goethite. *n* indicates the number of data points used for histogram

The histogram for galena displays a modal SI value of zero, whereas that for clausthalite is at SI ≈ -0.5. The SI histogram for cerussite (not shown) indicates that this mineral does not control Pb activity in most groundwaters under reducing conditions. However, a small

percentage, maybe 5%, of the selected potable groundwaters from the NWIS database could be saturated with respect to this mineral under conditions more oxidizing than those defined by the pyrite/goethite buffer.

Similar evaluations were also conducted with respect to the mineral hosts containing Hg, Sb, Se, U, and Zn (Birkholzer et al. 2008). Overall conclusions as to which minerals thermodynamically may control the activities of the selected hazardous elements in NWIS groundwaters are summarized in Table 2. Those minerals selected as trace elements hosts for further geochemical modeling (Sects. 3 and 4) are noted in bold in the table. The saturation indices for the candidate mineral hosts are consistent with moderately to strongly reducing conditions in at least 75% of all groundwater samples from the NWIS database, with the lower bound to the redox state most likely buffered by pyrite or another ferrous sulfide, and with some other mineral containing iron in either the Fe(II) or Fe(III) state. A small fraction of groundwaters, estimated to be perhaps as low as 5%, may be mildly reducing or even oxidizing. Table 2 recognizes the distinction

Table 2 Summary of minerals identified as controlling the thermodynamic activity of selected hazardous elements in potable groundwaters, those minerals selected as trace element hosts considered in Sects. 3 and 4 are noted in *bold*

Element	Thermodynamic control on groundwater activity		
	Moderately–strongly reducing, i.e., pyrite/goethite buffer	Mildly reducing–oxidizing	Comments
As	(1) **Arsenopyrite solid solution in pyrite (arsenian pyrite)** (2) Arsenopyrite	Adsorption on mineral surfaces, or through substitution for SO_4^{-2} in anionic clays such as green rust	No mineral in which As is an essential component, other than arsenopyrite, has been identified controlling arsenic activity in solution in the groundwaters examined
Ba	**Barite**	Barite	Barium activity is controlled by barite alone, regardless of oxidation state. No other Ba minerals controlling Ba activity have been identified
Cd	(1) **Greenockite solid solution in either sphalerite or galena** (2) Cadmoselite	Otavite	Greenockite is probably in solid solution in sphalerite and/or galena. The observed saturation with respect to cadmoselite suggests control of Cd^{+2} activity in some groundwaters for which Cd and Se analyses are available. Equilibrium concentrations in solution are so low, however, that current analytical methods are marginally effective in providing quantitative measurements. Under oxidizing conditions, cadmium activity is controlled by otavite. Otavite cannot be present in the majority of potable groundwaters analyzed for Cd in the NWIS database, because the aqueous Cd concentrations would then be easily detectable. This observation supports the conclusion that most groundwaters are reducing

Table 2 continued

Element	Thermodynamic control on groundwater activity		
	Moderately–strongly reducing, i.e., pyrite/goethite buffer	Mildly reducing–oxidizing	Comments
Hg	(1) **Cinnabar solid solution in pyrite** (2) Cinnabar (3) Tiemannite	Quicksilver	Majority of groundwaters equilibrate with respect to cinnabar (HgS) solid solution in pyrite. Both cinnabar and tiemannite might saturate in Hg-rich environments. Under mildly reducing environments, quicksilver saturation would be readily detected
Pb	(1) **Galena** (2) Clausthalite	Cerussite	A small fraction of groundwaters is sufficiently oxidizing that Pb activity is defined with respect to cerussite saturation. This observation supports the conclusion that most groundwaters are reducing. Pb mineralogy under mildly reducing–oxidizing conditions is complex. It is possible that secondary Pb silicates control Pb activity under these conditions
Sb	(1) **Gudmundite solid solution in pyrite** (2) **Kermesite (red antimony)**	Kermesite (red antimony)	Gudmundite solid solution in pyrite probably controls Sb concentration in most groundwaters. Under mildly reducing–oxidizing conditions, kermesite could control the Sb concentration
Se	(1) Dzharkenite solid solution in pyrite (2) Cadmoselite (3) Tiemannite (4) Clausthalite	None recognized	Se may substitute as the dzharkenite ($FeSe_2$) component in solid solution in pyrite, but if sufficiently abundant, may also stabilize as the selenide of Cd (cadmoselite), Hg (tiemannite), or Pb (clausthalite). No selenite or selenate minerals are recognized as activity controlling under mildly reducing–oxidizing conditions
U	(1) **Uraninite** (2) Coffinite	None recognized	Uranyl (UO_2^{+2}) minerals are strongly undersaturated, even when the redox state of the groundwater was specified by the goethite/Fe(II) defined Eh at a given pH
Zn	**Sphalerite**	Hemimorphite	Zinc carbonates, hydrozincite, and smithsonite are significantly undersaturated

between these two categories of groundwater, as defined broadly by their redox states. Of course, the claims presented are generalizations that apply to potable groundwaters of average composition and pH. These estimated average conditions are used to construct a geochemical model of general applicability for the geochemical simulations conducted as follows.

3 Variation of Aqueous Equilibrium Concentrations of Hazardous Elements with Partial Pressure of CO_2

In order to provide preliminary estimates of the potential magnitude of the impact of CO_2 intrusion into potable groundwater and to identify those trace elements most sensitive to CO_2

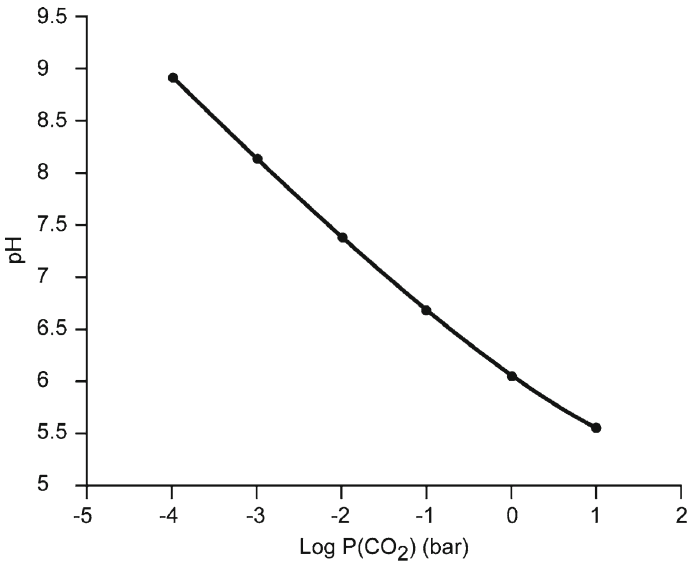

Fig. 6 Variation of pH with partial pressure of CO_2 under representative aquifer conditions at 25°C

intrusion, the aqueous equilibrium concentrations of each hazardous element were calculated as a function of the partial pressure of CO_2. Calculations were performed with EQ3/6 for a typical groundwater composition. The pyrite/goethite buffer at a given pH defined the redox state. The groundwater was also assumed to be saturated with respect to calcite, opal-CT, a low Fe–Mg smectite (specifying these minerals has negligible effect on predicted trace element concentrations), and the hazardous-element mineral hosts identified in Table 2 (selected minerals noted in bold). The partial pressure of CO_2 (in bar) was then imposed as a further equilibrium constraint and varied incrementally between log $P(CO_2) = -4$ and $+1$, the maximum range expected in shallow aquifers with hydrostatic pressure of up to 100 m. One effect of increasing $P(CO_2)$ is to shift pH downwards, as is illustrated in Fig. 6. However, the overall impact of increasing $P(CO_2)$ on the concentrations of hazardous trace elements varies is given further as follows.

It is important to understand the relationship between the thermodynamic model used to predict equilibrium concentrations of hazardous trace elements under specified CO_2 partial pressures and the observed concentrations of these same elements in NWIS groundwaters. The thermodynamic model was developed independently of the chemical analyses of NWIS groundwaters; it was used in the preceding section to evaluate the groundwater quality analyses and to determine the saturation state of minerals that might control the activities of the selected trace elements. The calculated modal SIs differ from the ideal value of zero by "closing errors" between model predictions and field measurements. These deviations are well within the overall uncertainty of the parameters relevant to the construction of the geochemical model, including the uncertainties and variabilities associated with the 38,000 chemical analyses of the NWIS groundwaters.

In order to ensure consistency with field observations and improve predictions of the likelihood that respective MCLs might be exceeded, we calibrated the geochemical model to the field data through adjustments to the solubility products of the respective mineral hosts. In other words, the final thermodynamic model used in this section, as well as in Sect. 4, was calibrated to the selected modes of the SI histograms calculated from the NWIS groundwater

analyses. The solubility products of galena, uraninite, and sphalerite, which control the concentrations of Pb, U, and Zn, respectively, were calibrated to ensure consistency between the modal concentrations of these elements and the thermodynamic model. Corrections were also made to the solubility products of arsenopyrite, cinnabar, gudmundite, and ferroselite (as a proxy for dzharkenite for which thermodynamic data are not currently available) to reflect the assumption that As, Hg, Sb, and Se substitute in solid solution in pyrite as FeAsS, HgS, FeSbS, and $FeSe_2$ components, respectively. The correction to the solubility product of greenockite is consistent with the assumed solid solution of CdS in sphalerite. In the case of Cd and Hg, where the majority of all water samples from the NWIS database have aqueous Cd and Hg concentrations too low to be detected with current state-of-the-art routine analytical methods, the magnitude of the calibration adjustment was based on the postulated modal concentrations, as discussed in Sect. 2.2.

The calibration process described above is justified in establishing estimates of the anticipated relative changes in the concentrations of the hazardous elements in response to increases in CO_2 partial pressure, especially in relation to the potential exceedance of their respective MCLs. Absolute model uncertainties lead to uncertainties in predictions of aqueous concentrations that are of an order of magnitude, a range that has limited value in providing regulatory guidance. From the scientific perspective, however, it is the absolute uncertainty that is of greater interest, as it is a measure of the model's ability to predict conditions in the natural environment. Results from the calculations of the saturation concentrations as a function of $P(CO_2)$, presented graphically in Fig. 7 for those elements that are sensitive to variations in $P(CO_2)$, therefore include both the calibrated predictions (in red), as well as the model estimates obtained without calibration of solubility products (in black). The figure also shows the estimated $\pm 1\sigma$ uncertainty band (shaded areas), on the basis of the cumulative uncertainties of the model as described in Birkholzer et al. (2008). Also included are the relevant MCLs, the detection limits for the most sensitive analytical methods, and an error bar indicating the observed or estimated natural variability of each element concentration as measured in the NWIS groundwater samples. The error bar illustrates the estimated $\pm 2\sigma$ variation about the mean of the log concentration of each trace element (± 1.5 log (mg/l)) at log $P(CO_2) \approx -2$, i.e., the average $P(CO_2)$ in NWIS groundwaters. The estimated $\pm 2\sigma$ variation about the mean is based on assumed lognormal distributions of Ba, U, and Zn, all of which give quantitative measurements for $\geq$90% of all samples. Note that Hg, Se, and U concentrations do not vary with $P(CO_2)$ and are not shown in Fig. 7. The aqueous species of these three elements are dominated, respectively, by neutral sulfide and selenide complexes (Hg, Se) and by UO_2(aq) (U), whose concentrations are independent of pH or $P(CO_2)$.

The predicted concentrations of some of the hazardous elements in Fig. 7 are sensitive to changes in $P(CO_2)$, whereas others remain relatively unaffected. Ba is slightly affected, but the maximum concentration (from the calibrated model) at elevated $P(CO_2)$ ($\approx$0.4 mg/l at 10 bar) remains below the MCL (maximum contaminant level) of 2 mg/l. Cd, Pb, and Zn show marked increases when log $P(CO_2)$ rises above -1. In the case of lead, the maximum calibrated concentration at elevated $P(CO_2)$ ($\approx$0.017 mg/l at 10 bars) slightly exceeds the MCL of 0.015 mg/l. The maximum calibrated concentration of zinc is also higher than the level suggested in the SDWR (i.e., 27 mg/l at 10 bar). Arsenic concentration changes strongly with increasing $P(CO_2)$, with a maximum calibrated concentration ($\approx$ 0.46 mg/l at 10 bar), significantly higher than the MCL for arsenic of 0.01 mg/l. Sb initially increases in parallel with As, then saturates with respect to kermesite at log $P(CO_2) > -2$, and thereafter remains at a concentration level significantly below the MCL of 0.006 mg/l. These differing behaviors are due to variations in pH and Eh as well as

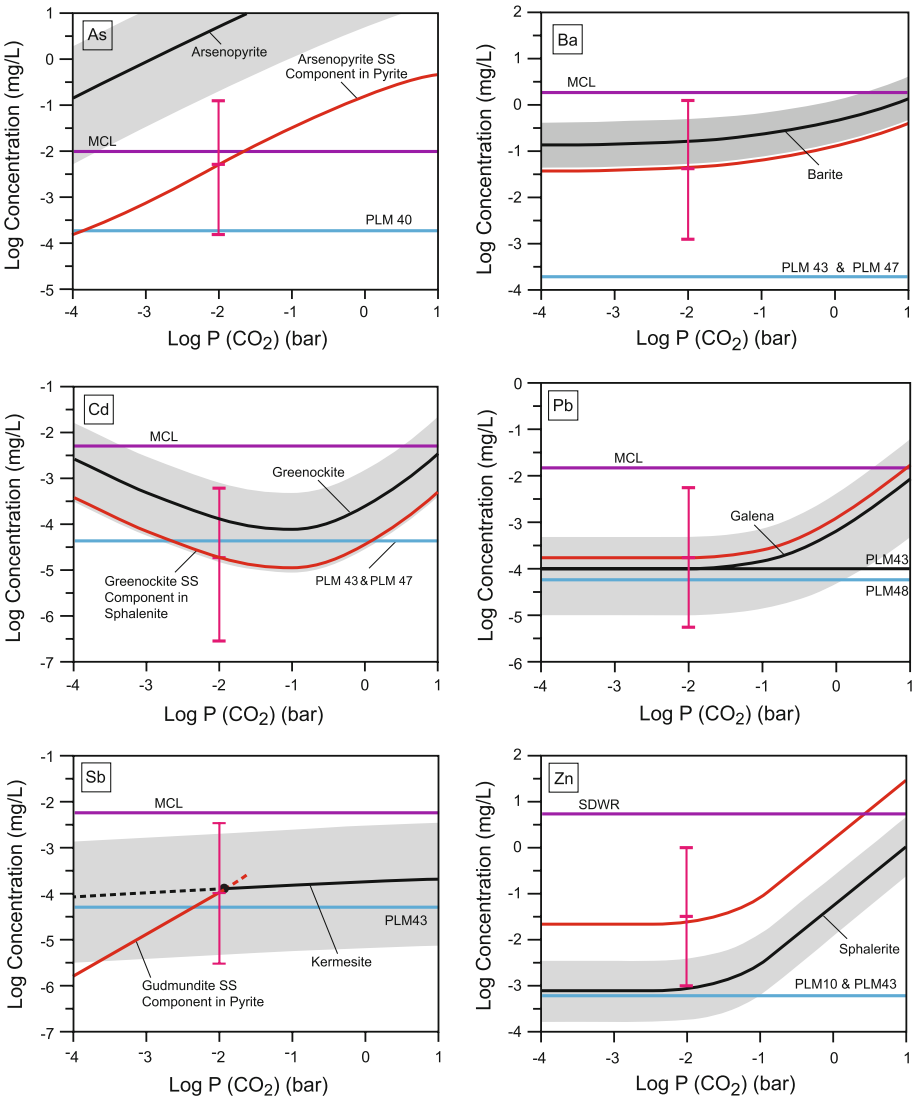

Fig. 7 Variation of trace metal concentrations in equilibrium with host minerals as a function of CO_2 partial pressure. The *black line with shaded* $\pm 1\sigma$ envelope represents model predictions obtained without calibration of solubility products. The *red line* and associated $\pm 2\sigma$ error bar represents the calibrated concentration based on the solubility products calibrated to ensure consistency with the modal concentrations of hazardous elements in NWIS waters. SS refers to solid solution. PLM10, PLM40, PLM43, PLM47, and PLM48 are analytical methods cited in the NWIS database. MCL signifies the maximum contaminant level for each element. SDWR stands for secondary drinking water regulation

to variations in the nature and distributions of complexes of each element in aqueous solution.

Our results suggest that the most serious water quality issue resulting from CO_2 intrusion may be the enhanced dissolution of arsenian pyrite with consequent solubilization of arsenic,

with a high probability that the MCL for arsenic would be exceeded at equilibrium with plausible $P(CO_2)$ levels representative of CO_2 intrusion into shallow potable aquifers. Pb and Zn may also exceed regulatory concentration limits; however, Zn is not considered hazardous according to EPA regulations. The focus of subsequent reactive-transport simulations in the next section is therefore on the mobilization and transport of As and Pb in potable water aquifers following intrusion of CO_2 from deep storage.

4 Reactive-Transport Modeling of CO_2 Intrusion into a Shallow Aquifer

A systematic modeling study was conducted with the reactive-transport simulator TOUGHREACT (Xu et al. 2006) considering a synthetic scenario with CO_2 intrusion into a shallow aquifer. The model starts with the basic assumption that CO_2 stored in deep geologic units can escape via preferential pathways, such as a fault zone, and enter the shallow aquifer locally from below at a constant rate. The reactive-transport model is used to predict the transport of gaseous and dissolved CO_2 within the shallow aquifer as well as the geochemical changes introduced by the presence of CO_2, in particular, the mobilization of arsenic and lead and their migration in the groundwater. The chemical reactions considered include aqueous complexation, mineral dissolution/precipitation, and adsorption/desorption via surface complexation. Various sensitivity studies have been conducted for different hydrological, geochemical, and mineralogical conditions, to (1) account (partially) for the range of conditions found in domestic potable aquifers and their host rocks, and (2) to evaluate the uncertainty associated with geochemical processes and model parameters (Birkholzer et al. 2008); for brevity, only a small subset of these studies can be presented here. The scenarios and conditions, in particular, those describing the geochemistry and mineralogy of potable aquifers, have been selected based on the geochemical model definition described in the previous sections.

The TOUGHREACT simulator was developed by introducing reactive chemistry into the existing framework of a non-isothermal, multiphase, multicomponent fluid and heat flow code (Pruess et al. 1999). A specific fluid property module for CO_2 sequestration was utilized that includes a comprehensive description of the thermodynamics and thermophysical properties of a $H_2O - NaCl - CO_2$ system. For the conditions assumed in this study, the intrusion of gaseous CO_2 into a freshwater aquifer is modeled as a two-phase flow system, with dissolution of CO_2 into water occurring instantaneously until equilibrium concentration is reached. Excess CO_2 migrates within the aquifer, driven mainly by buoyancy forces.

The geochemical model implemented in TOUGHREACT considers a variety of equilibrium and kinetic chemical reactions (Xu et al. 2006). The thermodynamic data incorporated in TOUGHREACT, originally based on a modified EQ3/6 database, were significantly modified and expanded within this study. As described in Appendix A, specific consideration has been given to the thermodynamic data of the metal-sulfide minerals and aqueous complexes as well as metal selenide minerals and aqueous complexes. A general form of rate law was used for kinetically controlled mineral dissolution and precipitation (Steefel and Lasaga 1994). Mineral reactive surface areas used in this study were taken from Xu et al. (2006, 2007), with the exception of those for illite, kaolinite, smectite, and goethite which were based on published BET surface areas (Bradbury and Baeyens 2005; Gu and Evans 2007; Lackovic et al. 2003; Muller and Sigg 1991). Kinetic rate parameters for most minerals were taken from Xu et al. (2006, 2007), derived from work by Palandri and Kharaka

Table 3 Specific surface area and site densities for main adsorbents

Absorbent	Specific surface area (m^2/g)	Site density (mol/m^2)		References
		Strong site	Weak site	
Goethite	14.7	1.76×10^{-6}	3.22×10^{-6}	Muller and Sigg (1991)
Kaolinite	14.73	2.2×10^{-6}	3.0×10^{-6}	Lackovic et al. (2003)
Illite	66.8	1.3×10^{-6}	2.27×10^{-6}	Gu and Evans (2007)
Smectite-Ca	56.38	4.77×10^{-8}	9.54×10^{-7}	Bradbury and Baeyens (2005)

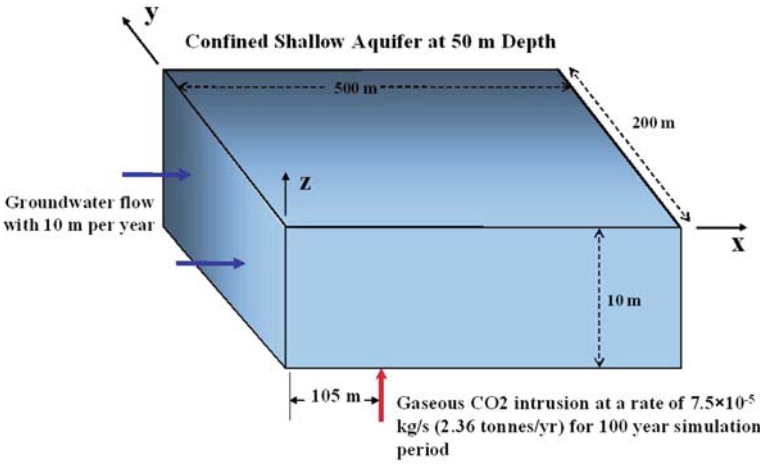

Fig. 8 Schematic representation for the setup of reactive-transport model

(2004). Kinetic rate parameters for arsenopyrite and galena were taken from Zhang et al. (2003).

Adsorption via surface complexation has been widely studied (Dzombak and Morel 1990; Lutzenkirchen 2006), and is a key process with respect to the fate and transport of heavy metals (for example, Bradl 2004) or other hazardous elements such as arsenic (Goldberg et al. 2005; Manning and Goldberg 1997). We have, therefore, incorporated into TOUGHREACT a model considering adsorption via surface complexation. Adsorption of heavy metal (and arsenic) ions on minerals is influenced by a variety of factors, the most important being pH, type and speciation of metal ion involved, competition between different ions (Bradl 2004), as well as specific surface area and site density of the adsorbing minerals. We considered goethite, illite, kaolinite, and smectite as principal adsorbents in this study, since these minerals have strong adsorption capacities with respect to lead and arsenic (see their specific surface areas and site densities in Table 3). A literature analysis was conducted to determine relevant surface complexation reactions and their thermodynamic constants for these cations and minerals.

Table 4 Mineral volume fractions and possible secondary minerals

Primary mineral	Volume fraction	Primary mineral	Volume fraction	Secondary mineral
Quartz	0.77	Pyrite	0.00512	Dolomite
K-feldspar	0.0618	Calcite	0.0151	Magnesite
Oligoclase	0.06	Goethite	0.00601	Ankerite
Kaolinite	0.017	Arsenopyrite SS	9.05×10^{-6}	Dawsonite
Smectite-Ca	0.0136	Galena	7.84×10^{-6}	Na-smectite
Illite	0.0285			Pyromorphite
Chlorite	0.0106			Ferroselite
Kerogen-OS	2.67×10^{-3}			Clausthalite

Note: SS = Solid solution

4.1 Model Setup

The model setup used for most of the simulations is depicted in Fig. 8. A confined shallow aquifer was considered with a uniform vertical thickness of 10 m at a reference depth of 50 m. The three-dimensional simulation domain comprises an area of this aquifer 500 m in length and 200 m in width. Water flows from left to right with a flow pore velocity of 10 m per year. Hydrogeologic properties are homogeneous and constant in time. Gaseous CO_2 enters the aquifer from below over an area of 100 m^2 (10 m × 10 m) at $x = 105$ m and $y = 0$ m, at a continuous rate of 7.5×10^{-5} kg/s, which corresponds to 2.36 tonnes per year. This rate was roughly based on the amount of CO_2 that can dissolve into the groundwater without forming a large two-phase zone of gaseous CO_2 and water. The aquifer is in a reducing environment, with a redox potential of approximately −0.23 V at pH around 7.6, defined by the coexistence of pyrite and goethite. The background level of log $P(CO_2)$ was set to approximately −2, consistent with the average partial pressure in NWIS groundwaters.

The host rock mineralogy, referred to as Coastal Plain Sandstone, is representative of an impure sandstone aquifer, based on considerations discussed in Birkholzer et al. (2008). Other mineralogies, representative of a range of domestic shallow aquifers, have also been considered in the simulation study, but results shall not be presented here. It is assumed that small volume fractions of minerals containing hazardous elements as essential components are present in the aquifers. Based on the findings from Sect. 2, the minerals that control the aqueous concentrations of As and Pb are arsenopyrite and galena, respectively (the former in solid solution in pyrite). The mineralogy of Coastal Plain Sandstone aquifer is listed in Table 4, including the major and minor minerals as well as clays.

Note that the volumetric fractions of hazardous-constituent-bearing minerals are typically too small to be measured with conventional petrologic analyses; information on their average abundances in aquifer host rocks was thus not generally available. Therefore, use was made of the National Geochemical Database (NGS) maintained by the United States Geological Survey, which contains the average elemental abundances in surficial soils and sediments in the United States. These abundances were then selected as a proxy for abundances in aquifer host rocks. The resulting volumetric fractions of the selected elements were further checked against two other referenced sources of elemental abundances: (a) calculated crustal abundances based on the averages of values presented by Wänke et al. (1984), Weaver and Tamey (1984), Shaw et al. (1985), Taylor and McLennan (1985), Earnshaw and Greenwood

Table 5 Initial total aqueous concentration of major constituents obtained by initial equilibrium run for the base model

Species	Concentration (mol/l)	Species	Concentration (mol/l)
Ca	9×10^{-4}	TIC	3.3×10^{-3}
Mg	2.2×10^{-5}	SO_4^{-2}	1.9×10^{-4}
Na	2×10^{-3}	Cl	2.1×10^{-4}
K	2.7×10^{-4}	Pb	1.3×10^{-9}
Fe	5.6×10^{-6}	As	4.4×10^{-8}
Si	9.3×10^{-4}	Ionic strength	0.0051

(1997), and Lide (2005), and (b) abundances in domestic coals (Bragg et al. 1998; USGS 2001; Golightly and Simon 2006). Average abundances of hazardous trace elements ranged from $<10^{-7}$ for Hg to $>10^{-4}$ for Ba (Birkholzer et al. 2008). While the above abundances are very small compared to the major minerals, all hazardous elements targeted in this study occur ubiquitously in soils, sediments, and aquifer rocks, indicating that the problem of mobilization of these elements in response to CO_2 intrusion could be widespread in United States aquifers.

4.2 Model Results

Equilibrium runs were conducted prior to simulating CO_2 intrusion to establish the initial chemical composition of the groundwater at equilibrium with the selected mineralogy (see Table 5). This initiation step also establishes equilibrium between mineral solubilities and adsorption sites, essentially "loading" these up. Note that the initial total aqueous concentrations of major and hazardous elements obtained from the initial equilibrium run are reasonably consistent with the peak values observed in the histograms from NWIS groundwater analyses. For example, the calculated initial concentration of total aqueous Pb concentration is 1.3×10^{-9} mol/l (2.7×10^{-4} mg/l), and the calculated initial concentration of total aqueous As concentration is 4.42×10^{-8} mol/l (3.3×10^{-3} mg/l), both of which falls close to the maximum frequencies observed in the NWIS analyses (see Fig. 2). Starting with the equilibrated initial conditions, the impact of CO_2 intrusion was modeled with the reactive-transport simulator TOUGHREACT. CO_2 intrusion starts at time zero and continues for the entire simulation period of 100 years.

4.2.1 Prediction of CO_2 Plume Evolution and Changes in Acidity

At the leakage rate of 7.5×10^{-5} kg/s, the CO_2 entering the aquifer dissolves effectively into the groundwater. A gas phase evolves after around 3 years close to the intrusion area and a small two-phase zone remains present during the remainder of the simulation period. The plume of elevated dissolved CO_2, which is given by total inorganic carbon (TIC), migrates from the two-phase zone primarily along the groundwater flow direction, while lateral spreading of dissolved CO_2 is minor (Fig. 9a). The evolution of pH follows closely the evolution of TIC, with pH decreasing as the concentration of TIC rises (Fig. 9b). The lowest pH is around 5.7 within and about 5.9 outside of the two-phase zone (compared to an initial pH of 7.6), both of which are higher than the expected pH in a system without any buffering minerals. (For a non-buffered system, a pH around 4.5 would be expected). The moderation in pH decrease is caused primarily by the dissolution of calcite.

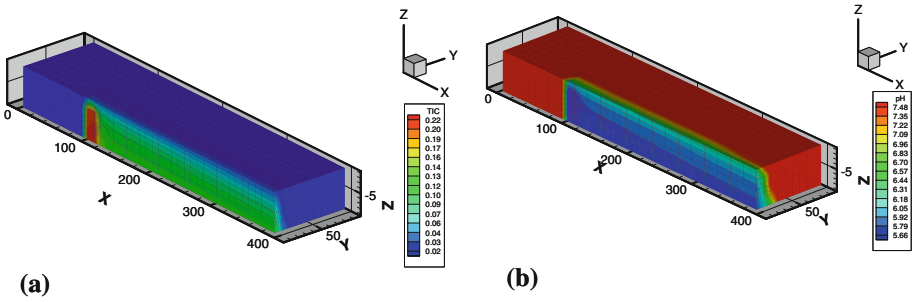

Fig. 9 Spatial distribution of (**a**) Total Inorganic Carbon (in mol/l) and (**b**) pH after 100 years. CO_2 intrusion rate is 7.5×10^{-5} kg/s

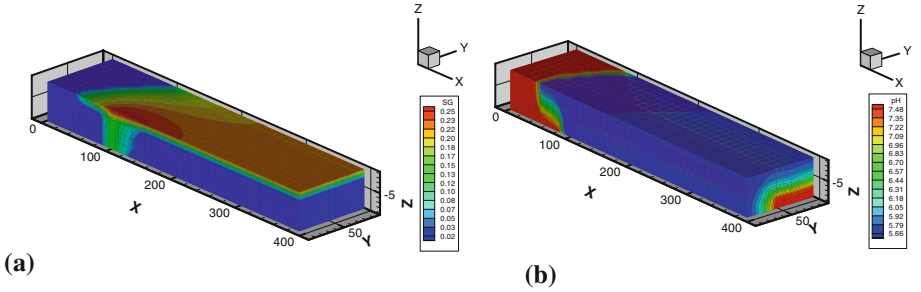

Fig. 10 Spatial distribution of (**a**) CO_2 gas saturation and (**b**) pH after 100 years. CO_2 intrusion rate is 6×10^{-4} kg/s

The spatial evolution of gaseous as well as dissolved CO_2 strongly depends on the CO_2 intrusion rate and the groundwater flow velocity. For illustration, Fig. 10a shows model results of CO_2 gas saturation after 100 years of CO_2 intrusion with a higher intrusion rate of 6×10^{-4} kg/s. Since the amount of CO_2 entering the aquifer clearly exceeds the dissolution capacity of the groundwater, most of the leaking CO_2 remains in the gas phase, migrates upward until it reaches the upper closed boundary of the confined aquifer, and spreads out laterally, bypassing most of the groundwater body. The plume of increased acidity (Fig. 10b) is influenced by the spatial extent of gaseous CO_2 as well as the advective–dispersive transport of CO_2-charged water. Notice that the lowest pH levels are similar to those obtained in the previous case. Once the CO_2 reaches its solubility limit, there is no further increase in TIC and acidity. Similar buoyancy effects occur in a sensitivity case with lower groundwater flow velocity (not shown here). Dissolution of CO_2 is less effective in this case because less water undersaturated with respect to CO_2 flows toward the intrusion zone.

4.2.2 Prediction of As and Pb Concentrations

With increasing acidity, contaminants can be mobilized from the aquifer rocks via mineral dissolution and desorption from mineral surfaces. As a result, elevated aqueous Pb and As concentrations are predicted to occur in response to the observed TIC and pH changes. The aqueous As concentrations depicted in Fig. 11 follow closely the spatial distribution of elevated TIC and lower pH shown in Figs. 10a and b. Comparison between the concentration distributions in Fig. 11 demonstrates that the rate of CO_2 entering an aquifer has a significant

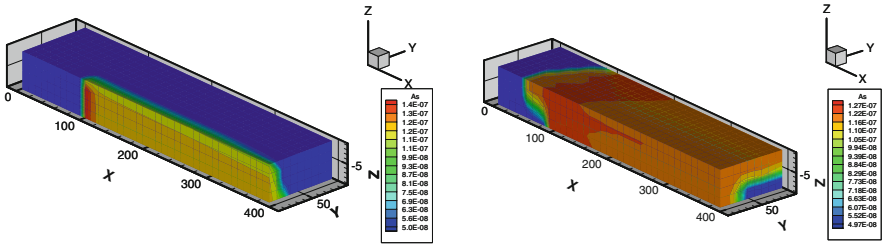

Fig. 11 Spatial distribution of total aqueous As concentration after 100 years. CO_2 intrusion rates are (**a**) 7.5×10^{-5} kg/s and (**b**) 6×10^{-4} kg/s

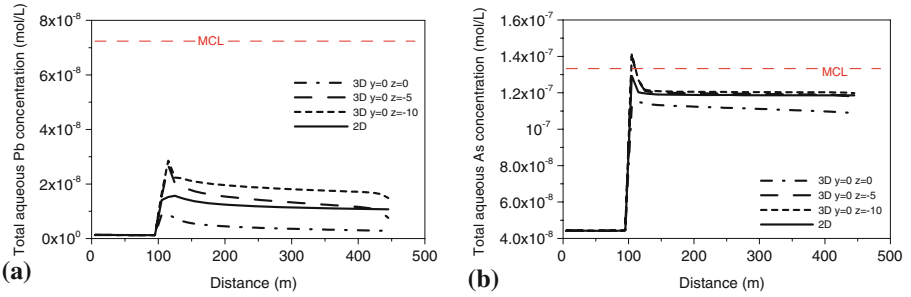

Fig. 12 Concentration profiles along x-axis at $y = 0$ m and different aquifer depths ($z = 0, -5$, and -10 m) for 3D model. **a** Total aqueous Pb concentration. **b** Total aqueous As concentration. CO_2 intrusion rate is 7.5×10^{-5} kg/s. Also shown are profiles from a 2D depth-averaged model

impact on the spatial distribution of groundwater contamination, but only a minor effect on the maximum contaminant levels. This is consistent with the observation that the lowest pH levels are slightly affected by the CO_2 intrusion rate.

The processes that control the changes in aqueous As and Pb concentration in response to CO_2 intrusion include dissolution/precipitation of host minerals, desorption/adsorption, and dissociation/association of aqueous complexes. The resulting concentrations are furthermore affected by complex transient interaction between these processes, as discussed in the following for the case with a CO_2 intrusion rate of 7.5×10^{-5} kg/s. Figure 12a and b show Pb and As concentration after 100 years in profiles, respectively, along the x-axis at different elevations within the 10-m thick aquifer. The profiles intersect the location where CO_2 enters the aquifer ($y = 0$ m). Also, Fig. 12 shows the simulation results from a 2D model, which neglects the vertical variation. The predicted As and Pb concentrations obtained with the 2D model are in reasonable agreement with those from the 3D model.

The peak value of aqueous Pb in Fig. 12a is 2.7×10^{-8} mol/l (0.006 mg/l) in the small two-phase zone at the injection location after 100 years at the bottom of aquifer ($z = -10$ m). The aqueous Pb concentration downstream approaches a stable value around 2×10^{-8} mol/l (0.004 mg/l) at the bottom of aquifer. This value is significantly higher (about 15 times) than the initial concentration, but remains below the MCL, which is 7.24×10^{-8} mol/l (0.015 mg/l). Slightly lower concentrations are observed in the middle and at the top of the aquifer.

We have evaluated the transient changes in galena volume fraction as well as the total Pb concentrations on adsorption sites to assess the relative importance of different mobilization processes. In the case of lead, desorption of the Pb^{+2} ion from mineral surfaces turns out to

be more relevant than dissolution of galena. The ingress of CO_2 immediately disturbs both adsorption and solubility equilibria, but whereas adsorption reactions re-equilibrate almost instantaneously, the dissolution/precipitation of the hazardous mineral host is kinetically controlled and typically much slower. The relatively sudden release of Pb from adsorption sites increases the aqueous Pb concentration in the two-phase zone near the intrusion location so significantly that the solution actually supersaturates with respect to galena and galena precipitation occurs. Further increases of Pb concentrations downstream of the two-phase zone are limited because the aqueous Pb arriving from upstream sorbs back on the mineral surfaces. The way that these processes—desorption/adsorption and galena dissolution/precipitation—interact with each other is governed by the kinetic rate of galena dissolution/precipitation, galena solubility as a function of $P(CO_2)$, the total number of adsorption sites on mineral surfaces, and the surface complexation constants.

The resulting As concentrations in Fig. 12b are consistent with the equilibrium calculations in Sect. 3, and suggest a greater likelihood of impacts on water quality than is the case for Pb. The maximum concentration of aqueous As reaches the MCL (1.33×10^{-7} mol/l or 0.01 mg/l) within the small two-phase zone, and is slightly lower (about 1.2×10^{-7} mol/l or 0.009 mg/l) than the MCL within the elongated area of increased acidity downstream of the intrusion location. In contrast to the Pb observations, where the metal-hosting mineral (galena) actually precipitates after intrusion of CO_2, arsenic in the two-phase zone is mobilized by both desorption and by dissolution of arsenopyrite solid solution. Further downstream, the dissolution of arsenopyrite becomes less effective, and aqueous As sorbs back onto the mineral surfaces, limiting further concentration increases.

The differences in the mobilization behavior of Pb and As in response to CO_2 intrusion—desorption combined with galena precipitation in the case of Pb compared to desorption and arsenopyrite dissolution in the case of As—point to the complexities involved in reactive-transport modeling and the interplay between the various processes involved. For example, as shown in Fig. 7, the solubility of arsenopyrite increases more significantly with the partial pressure of CO_2 than the solubility of galena, because sulfide and selenide complexation effectively inhibits $PbCO_3(aq)$ complexation. This is one of the main reasons why the desorption of As does not cause supersaturation with respect to the pre-existing arsenopyrite solid solution, while the desorption of Pb causes supersaturation with respect to galena. However, variations in the kinetic rates or changes in other geochemical parameters may affect these simulated trends.

The mobilization of Pb and As from mineral dissolution and from adsorption sites causes only very small changes to the initial contaminant mass in the solid phase, even after 100 years of CO_2 intrusion. For example, although the initial volume fraction of arsenopyrite in the aquifer is very small, on the order of 10^{-5} of the total mineral volume, this mineral is far from being depleted after 100 years of increased acidity. Very small amounts of Pb and As contained in the aquifer solid phase can thus provide a long-lasting source of contamination.

4.3 Sensitivity Analyses

A series of sensitivity analyses has been conducted with respect to geochemical processes, model setup, initial and boundary conditions, only one of which is presented below. Sensitivities to many other parameters and processes—such as host rock (major and minor) mineralogy, solubility, kinetic rate, aqueous complexation constant, initial partial pressure of CO_2, depth of aquifer, and redox conditions—are evaluated in Birkholzer et al. (2008). Note

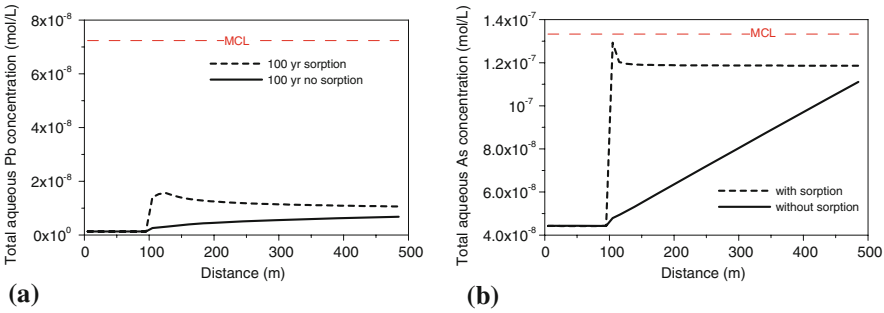

Fig. 13 Comparison of model results from sensitivity run (without sorption) with base model (with sorption). Concentration profiles from 2D depth-averaged model along x-axis at $y = 0$ m. **a** Total aqueous Pb concentration. **b** Total aqueous As concentration. CO_2 intrusion rate is 7.5×10^{-5} kg/s

that all sensitivity analyses were run with a 2D model, considering a 10 m/year groundwater velocity and a CO_2 intrusion rate of 7.5×10^{-5} kg/s.

The base-model results discussed in the previous section suggest strongly that adsorption/desorption and mineral dissolution/precipitation act together as the most important processes that control the evolution of aqueous As and Pb. Previous study on the subject by Wang and Jaffe (2004) did not consider adsorption/desorption processes. Therefore, to explore the role of adsorption/desorption, we conduct a run without adsorption/desorption and, in Fig. 13, compare the resulting lead and arsenic concentrations after 100 years with the previously obtained results.

In the base model, desorption in the two-phase zone releases Pb into the aqueous phase, and the solution becomes supersaturated with respect to galena and its precipitates. In the sensitivity run, the increased acidity due to the ingress of CO_2 causes dissolution of galena. Aqueous Pb mobilized close to the injection zone migrates downstream, where galena continues to dissolve due to the lowered pH. As a result, the initially relatively small aqueous Pb concentrations continue to buildup with travel distance (Fig. 13a). The trend observed in the profile is moderate, and it is not clear whether lead concentrations above the MCL could be reached much further downstream should the travel interval be sufficient long.

The omission of adsorption/desorption processes is similarly important for arsenic. Without adsorption, the arsenic concentrations increase significantly with travel distance (Fig. 13b). The trend seen in the profiles suggests strongly that the MCL for arsenic would continued to increase and eventually be exceeded further downstream until the equilibrium limit is reached. This is in contrast to the base model, where adsorption stabilizes the aqueous As concentrations downstream of the intrusion location to a relatively uniform level that is smaller than the MCL. The base-model results also show much higher concentration values in the two-phase zone near the CO_2 intrusion location, which are caused by the significant mobilization of initially adsorbed As.

These results indicate that adsorption/desorption via surface complexation is arguably the most important process controlling the fate of hazardous elements mobilized by CO_2 leakage when adsorbing minerals are present. Without adsorption, the resulting long-term contamination of an aquifer would be less significant near the region where CO_2 enters, whereas aqueous concentrations would keep increasing with travel distance, as acidic water migrates further and more dissolution occurs. Furthermore, the dissolution or precipitation of galena and arsenopyrite is a very slow process, whereas adsorption/desorption reactions equilibrate

almost instantaneously. Thus, desorption of initially adsorbed matter is the dominant process in mobilizing contaminants in the short term.

5 Concluding Remarks

This article describes a systematic evaluation of the possible water quality changes in response to CO_2 intrusion into aquifers currently used as sources of potable water in the United States. Three main tasks were conducted: (1) to develop a comprehensive geochemical model representing typical conditions in many freshwater aquifers and, for those conditions, to determine likely host minerals controlling the concentrations of hazardous elements in potable groundwaters; (2) to conduct a thermodynamic equilibrium analysis identifying those hazardous elements most likely to be mobilized as a result of mineral dissolution associated with elevated $P(CO_2)$ levels; and (3) to perform reactive-transport modeling to quantify the effect of CO_2 intrusion into shallow aquifers.

Considering a representative groundwater under reducing conditions, our results show that CO_2 leakage into a shallow aquifer can lead to long-lasting mobilization of hazardous trace elements, in particular arsenic and lead, near the intrusion location and farther downstream. Our thermodynamic equilibrium calculations identified As and Pb as those trace elements with the highest potential for exceeding regulatory water quality limits at elevated CO_2 concentrations. However, while the reactive-transport model also suggests substantial increases in aqueous concentrations as a result of CO_2 intrusion, the predicted As concentration only slightly (and locally) exceed the MCL for arsenic in groundwater, whereas the MCL for Pb is exceeded under the simulated conditions. Our results furthermore indicate that adsorption/desorption via surface complexation is a very important process controlling the fate of hazardous elements mobilized by CO_2 leakage when adsorbing minerals are present.

As stated before, the goal of our generic study was to better understand, in a global sense, the vulnerability of representative and relevant aquifer types in the case of CO_2 intrusion. A comprehensive sensitivity study was, therefore, conducted for different hydrological, geochemical, and mineralogical conditions (Birkholzer et al. 2008), only a small subset of which could be presented here. It is understood that even the most comprehensive sensitivity study can neither encompass all possible conditions and scenarios, nor can it account for all relevant uncertainties. We recommend that the generic study should be followed up with site-specific model predictions, and that laboratory or field experiments should be performed to test uncertain model assumptions and parameters. Such experiments would involve exposing initially undisturbed groundwater in laboratory samples or in situ in the field to elevated levels of CO_2.

One of the principal findings of this study is that most potable groundwaters sampled in the United States, are reducing, and that minerals containing the investigated hazardous trace elements are, for all but Ba, stable only under reducing conditions. This finding may be controversial, and it is, therefore, important that further studies be conducted to test the claims asserted in this article. While the authors are confident that the supporting evidence is strong, and, taken in its entirety, convincingly supports our findings as a general rule, some details may require amendment or revision upon further analysis. Of particular importance is the correct identification of the mineral hosts. Of necessity, these had to be inferred, as direct detection has not been attempted in potable water aquifer host rocks, and would be exceedingly difficult under normal conditions. Should other, presently unidentified minerals control the aqueous concentration of certain of the trace elements in potable groundwaters, the response to changing $P(CO_2)$ could differ from that predicted

in this article. Furthermore, with respect to Cd, Hg, Sb, and Se, our analysis could not infer with complete confidence whether pure substances or solid solutions are controlling, or whether both are involved due to natural variability in host rock chemical and mineralogical composition. Phase metastability, caused by small particle size, or solid solution instability, induced by changing temperature, could also modify responses of mineral hosts to CO_2 intrusion. Many other uncertainties, both in the conceptual model and in the thermodynamic data used in the model, require resolution, and should be the basis for fruitful and challenging study. Perhaps the greater contribution of this article will not be so much in the conclusions reached, as in the stimulus it provides for investigating further the questions posed.

Acknowledgments We thank the U.S. Environmental Protection Agency, Office of Water and Office of Air and Radiation, for funding this study under an Interagency Agreement with the U.S. Department of Energy at the Lawrence Berkeley National Laboratory, under Contract Number DE-AC02-05CH11231. We also gratefully acknowledge the assistance provided by Jonathon C. Scott, U.S. Geological Survey, Oklahoma City, Oklahoma, in extracting and supplying approximately 38,000 groundwater analyses from the NWIS database. We are most appreciative of the careful and thorough reviews conducted by Yousif Kharaka and an anonymous reviewer. Their suggestions have helped greatly in improving both the clarity and precision of the article.

Appendices

Appendix A: Modification and Augmentation of the Thermodynamic Database Supporting the EQ3/6 Code

The EQ3/6 code contains a database, Data0.dat, which is a compilation of solubility products and dissociation constants for minerals and aqueous species, respectively. In order to accommodate the requirements of the current study, we revised, reconciled, and augmented the database using experimentally determined thermochemical data recently reported in the literature, details of which are given in Birkholzer et al. (2008). One of the most important aspects relating to modification of the EQ3/6 database resulted from the realization that the intrinsic solubilities of sulfides of Cd, Fe, Hg, Pb, and Zn are governed by the presence of ill-characterized oligomeric neutral sulfide complexes in solution, and that these must be accounted for to reconcile solubility measurements for these sulfides with the corresponding experimentally determined enthalpies of formation. Figure 14a illustrates a derived linear correlation between the logarithms of the solubility products, $\mathrm{Log}K_s$, of the crystalline metal monosulfide and the corresponding logarithms of the dissociation constants, $\mathrm{Log}K_{aq}$, for the neutral sulfide complexes, respectively, defined by the reactions:

$$\mathrm{MeS(s)} + \mathrm{H^+} = \mathrm{Me^{+2}} + \mathrm{HS^-} \tag{A.1}$$

$$\mathrm{MeS(aq)} + \mathrm{H^+} = \mathrm{Me^{+2}} + \mathrm{HS^-} \tag{A.2}$$

This correlation is based on thermochemical data from Robie and Hemingway (1995) and Rickard (2006) for the solids, and Dyrssen (1988, 1989) for all sulfide complexes, except HgS(aq), which was taken from Dyrssen and Wedborg (1991). The large measure of agreement obtained with this correlation permitted inclusion of dissociation constants for neutral sulfide complexes for Cd, Fe, Hg, Pb, and Zn in the EQ3/6 database.

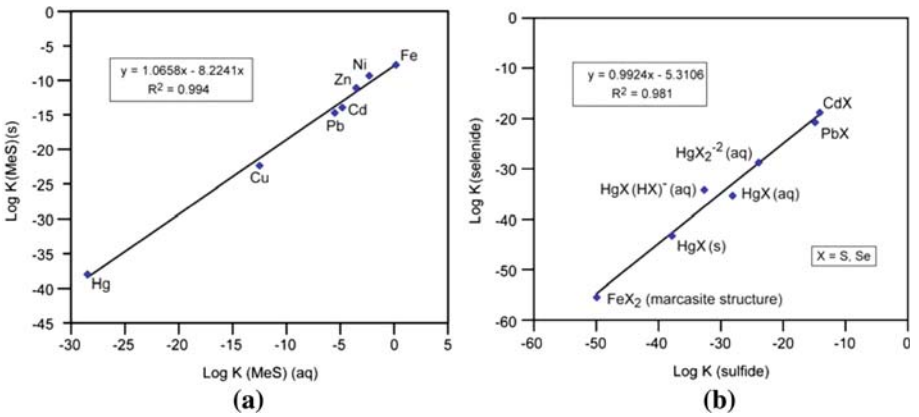

Fig. 14 Correspondence plots to show the correlation between (**a**) the dissociation constants of oligomeric neutral sulfide complexes and the monosulfides of selected hazardous trace elements, and (**b**) sulfides and selenides of selected hazardous trace elements, and the aqueous sulfide and selenide complexes of Hg

It was also recognized that similar oligomeric selenide neutral complexes of these same elements must be present in solution, which in some cases contribute significantly to enhanced concentrations of the corresponding metals. Information on selenide complexes of the metals of interest is limited to the study by Mehra and Gubeli (1971) on Hg selenide complexes. A correspondence plot of the respective the logarithms of the solubility products, $\mathrm{Log}K_s$, of the crystalline metal monosulfide and the corresponding logarithms of the dissociation constants, $\mathrm{Log}K_{aq}$, for the Hg sulfide complexes, when plotted against the corresponding selenide species, also yielded a linear correlation as illustrated in Fig. 14b. The data used in this plot was derived from thermochemical data given by Robie and Hemingway (1995) and from the EQ3/6 Data0.dat database for the solid phases, and from Paquette and Helz (1997) and Mehra and Gubeli (1971) for aqueous Hg sulfide and selenide complexes, respectively. The linear correlation was used to estimate dissociation constants of the relevant selenide complexes for, Cd, Fe, Pb, and Zn. Further details concerning the methods used and assumptions made in deriving the required solubility products and dissociation constants are discussed in Birkholzer et al. (2008). For consistency, we made similar modifications to the database employed by the reactive-transport TOUGHREACT (Xu et al. 2006) used in Sect. 4.

We omitted to take into account organic complexation of the selected hazardous metals, because the concentrations of dissolved organic complexants in groundwaters used for drinking water are relatively low, and because mineralization further mitigates their impact. Furthermore, as noted by Rozan et al. (2003), complexation by oligomeric neutral sulfide complexes incorporated in our geochemical model, are, at least for Pb, so strong that they overwhelm organic complexation under reducing conditions. We acknowledge, however, that further study of this question is merited, especially in relation to Hg, e.g., see Paquette and Helz (1997) and Skyllberg (2008).

Appendix B: Evaluation of Groundwater Redox State

Estimating the redox potential of groundwaters is critical to the interpretation of most hazardous elements targeted in this study. Elements such as As, Hg, Sb, Se, and U occur in differing oxidation states that are stable in the presence of water. Also, As, Cd, Hg, Sb,

Pb, and Zn commonly form insoluble sulfides under reducing conditions, which become unstable under oxidizing conditions, where sulfur is oxidized from -II or -I to the 0, II, IV, or the VI state. Furthermore, As, Hg, Sb, and Se can substitute in the pyrite lattice, which is destabilized under oxidizing conditions. Some of the hazardous elements can also form compounds with each other, e.g., selenides of As, Cd, Hg, Pb, or Zn, or arsenates of Pb. Thus, a variety of solubility-controlling minerals can form, depending mainly on both the pH and the redox state of the groundwater. Although measurements using a Pt electrode can be used to indicate the redox state, or Eh, of a groundwater, such measurements are subject to error and misinterpretation (Baas Becking et al. 1960; Lindberg and Runnels 1984; Fish 1993; Stefansson et al. 2005), and more commonly provide only an indication of the mixed potential of a non-equilibrated system. For example, not all species of an element that can occur in different oxidation states are necessarily in redox equilibrium, as has been observed with respect to As(III)/As(V) (Cherry et al. 1979; Johnston and Singer 2007), Sb(III)/Sb(V), Se(II)/(IV)/Se(VI), and S(II)/S(VI) (Sato 1992).

Instead of relying on direct Eh measurements of questionable reliability and limited availability, we tested alternative methods of indirectly estimating redox state. The first involved the recognition that equilibration between Fe(II) and Fe(III) occurs relatively rapidly in the aqueous phase (Grundl and Macalady 1989), which allows calculating the Eh at a given pH using measurements of these species. Our assumption was that the Fe(III) concentration in solution is in equilibrium with a ferric oxide or oxyhydroxide, and that any Fe(total) in excess would be present as Fe(II). Over 20,000 of the analyses extracted from the NWIS database contain Fe measurements, providing a solid basis for calculating the probable Eh of a significant fraction of all samples. The calculated distributions of mineral SIs identified as potential mineral hosts (Table 1) showed that a very large scatter and exhibited results that were inconsistent with the posited modes of occurrence of the studied trace elements. Therefore, we ran an alternative test, where it was assumed that the redox state was dominantly controlled by the pyrite/goethite buffer at a given pH. The resulting calculated distributions of mineral host SIs showed considerably less dispersion, and were consistent with the observed modes of occurrence discussed above. We therefore decided to conduct the thermodynamic evaluation of all trace element SIs using the alternative assumption, i.e., that the pyrite/goethite buffer controls Eh at any measured pH. However, we recognize that other mineral Eh buffers could be operative and that some portion of the analyses may represent groundwaters with higher Eh values.

Implicit in the assumption that goethite and pyrite are in thermodynamic equilibrium is that sulfide and sulfate species in solution are also in thermodynamic equilibrium, which conflicts with the widely held belief that these species are practically never in equilibrium in groundwaters. This belief is not, however, supported by Washington et al. (2004), who characterized the redox chemistry of three shallow aquifers in Georgia in exquisite detail. Their study showed that redox pairs aggregated into two clusters in local partial equilibrium, an upper pe cluster containing N, Fe, and O_2/H_2O_2 couples, and a lower pe cluster consisting of C, S, and H couples. The former appears to be determined mainly by the presence of NO_3^- in relation to reduced N species (NO_2^-, N_2O, N_2, NH_4^+) and controls Fe(III)ppt/Fe(II), whereas the latter includes SO_4/H_2S and H_2CO_3/CH_4, and is mainly controlled by decomposing organic matter. Because most of the candidate hazardous-element mineral hosts are chalcogenides, it is reasonable to assume that their saturation state is determined in part by SO_4/H_2S, which falls a little below the pyrite/goethite buffer at near neutral pH and equimolar concentrations of SO_4^{-2} and H_2S. Therefore, we have a ready explanation why the results of our evaluation were coherent with respect to pyrite/goethite, but not Fe(III)ppt/Fe(II). In addition, Washington et al. (2004) noted that with the depletion of NO_3 and intermediate

products of NO_3 reduction, the Fe(III)ppt/Fe(II) couple drifts progressively toward the lower pe cluster as homogeneous thermodynamic equilibrium in the aqueous phase is approached. Thus, we also have an explanation for the broad distribution of calculated Eh values, when Eh is calculated from Fe(III)ppt/Fe(II) at a given pH as shown in Birkholzer et al. (2008). Furthermore, the decay of organic matter can induce reducing conditions so low that both hydrogen and methane can be generated in shallow aquifers, where organic matter is translocated from overlying soil horizons, or is already present in sediments in which organic matter is trapped during accumulation. Such conditions, defined by H_2CO_3/CH_4, approach those associated with coal beds.

References

Aravena, R., Wassenaar, L.I., Plummer, L.N.: Estimating ^{14}C groundwater ages in a methanogenic aquifer. Water Resour. Res. **31**(9), 2307–2317 (1995)

Baas Becking, L.G.M., Kaplan, L.R., Moore, D.: Limits of the natural environment in terms of pH and oxidation–reduction potentials. J. Geol. **68**, 243–284 (1960)

Bachu, S.: Sequestration of CO_2 in geological media: criteria and approach for site selection in response to climate change. Energy Convers. Manag. **42**, 953–970 (2000)

Benoit, J.M., Gilmour, C.C., Mason, R.P., Wheyes, A.: Sulfide controls on mercury speciation and bioavailability to methylating bacteria in sediment pore waters. Environ. Sci. Technol. **33**, 951–957 (1999)

Birkholzer, J., Apps, J.A., Zheng, L., Zhang, Y., Xu, T., Tsang, C.-F.: Research project on CO_2 geological storage and groundwater resources: water quality effects caused by CO_2 intrusion into shallow groundwater. Lawrence Berkeley National Laboratory Technical Report, LBNL-1251E, 450 p. (2008). Available online at: http://www.osti.gov/bridge/product.biblio.jsp?query_id=0&page=0&osti_id=944435

Bradbury, M.H., Baeyens, B.: Modelling the sorption of Mn(II), Co(II), Ni(II), Zn(II), Cd(II), Eu(III), Am(III), Sn(IV), Th(IV), Np(V) and U(VI) on montmorillonite: linear free energy relationships and estimates of surface binding constants for some selected heavy metals and actinides. Geochim. Cosmochim. Acta **69**(4), 875–892 (2005)

Bradl, H.B.: Adsorption of heavy metal ions on soils and soils constituents. J. Colloid Interface Sci. **277**, 1–18 (2004)

Bragg, L.J., Oman, J.K., Tewalt, S.J., Oman, C.L., Rega, N.H., Washington, P.M., Finkelman, R.B.: The U.S. Geological Survey Coal Quality (COALQUAL) Data-Base, Version 2.0. U.S. Geological Survey Open-File Report 97-134, One CD-ROM (1998)

Carroll, S., Hao, Y., Aines, R.: Transport and detection of carbon dioxide in dilute aquifers. Proceedings 9th International Conference on Greenhouse Gas Control Technologies, November 2008, Washington, DC (2008)

Cherry, J.A., Shaikh, A.V., Tallman, D.E., Nicholson, R.V.: Arsenic species as an indicator of redox conditions in groundwater. J. Hydrol. **43**, 373–392 (1979)

Cooper, D.C., Morse, J.W.: Selective extraction chemistry of toxic sulfides in sediments. Aquat. Geochem. **5**, 87–97 (1999)

Davies-Colley, R.J., Nelson, P.O., Williamson, K.J.: Sulfide control of cadmium and copper concentrations in anaerobic estuarine sediments. Mar. Chem. **16**, 173–186 (1985)

Dyrssen, D.: Sulphide complexation in surface seawater. Mar. Chem. **24**, 143–153 (1988)

Dyrssen, D.: Biogenic sulfur in two different marine environments. Mar. Chem. **28**, 241–249 (1989)

Dyrssen, D., Wedborg, M.: The sulphur–mercury system in natural waters. Water Air Soil Pollut. **56**, 507–519 (1991)

Dzombak, D.A., Morel, F.M.M.: Surface Complexation Modeling: Hydrous Ferric Oxide. Wiley, New York (1990)

Earnshaw, A., Greenwood, N.: Chemistry of the Elements, 2nd edn. Butterworth-Heinemann, Oxford, UK, ISBN 0-7506-3365-4, Appendix 4, Abundance of Elements in Crustal Rocks (1997)

Edmunds, W.M., Bath, A.H., Miles, D.L.: Hydrochemical evolution of the East Midlands Triassic sandstone aquifer, England. Geochim. Cosmochim. Acta **46**, 2069–2081 (1982)

Finkelman, R.B.: Modes of occurrence of trace elements in coal. U.S. Geological Survey Open-File Report 81-99, p. 301 (1981)

Fish, W.: Sub-surface redox chemistry: a comparison of equilibrium and reaction-based approaches. In: Allen, H.E., Perdue, E.M. (eds.) Metals in Groundwater, Chap. 3. Lewis, Boca Raton (1993)

Focazio, M.J., Tipton, D., Dunkle Shapiro, S., Geiger, L.H.: The chemical quality of self-supplied domestic well water in the United States. Ground Water Monit. Remediat. **26**(3), 92–104 (2006)
Goldberg, S., Lesch, S.M., Suarez, D.L., Basta, N.T.: Predicting arsenate adsorption by soils using soil chemical parameters in the constant capacitance model. Soil Sci. Soc. Am. J. **69**(5), 1389–1398 (2005)
Golightly, D.W., Simon, F.O. (eds.): Methods for sampling and inorganic analysis of coal. U.S. Geological Survey Bulletin 1823 (2006)
Grundl, T.J., Macalady, D.L.: Electrode measurements of redox potential in anaerobic ferric/ferrous chloride systems. J. Contam. Hydrol. **5**, 97–117 (1989)
Gu, X., Evans, L.J.: Modelling the adsorption of Cd(II), Cu(II), Ni(II), Pb(II), and Zn(II) onto Fithian illite. J. Colloid Interface Sci. **307**, 317–325 (2007)
Hopkins, J., Putnam, P.: Fabric alteration and isotopic signature of carbonates in a recharge area of the Madison Aquifer, Montana, USA. J. Geochem. Explor. **69–70**, 235–238 (2000)
Huerta-Diaz, M.A., Morse, J.W.: Pyritization of trace metals in anoxic marine sediments. Geochem. Cosmochim. Acta **56**, 2681–2702 (1992)
Johnston, R.B., Singer, P.C.: Solubility of symplesite (ferrous arsenate): implications for reduced groundwaters and other chemical environments. Soil Sci. Soc. Am. J. **71**, 101–107 (2007)
Kharaka, Y., Cole, D.R., Hovorka, S.S., Gunther, W.D., Knauss, K.G., Freifeld, B.M.: Gas-water-rock interactions in Frio formation following CO_2 injection: Implications for the storage of greenhouse gases in sedimentary basins. Geology **34**, 577–580 (2006)
Kolker, A., Mroczkowski, S.J., Palmer, C.A., Dennen, K.O., Finkelman, R.B., Bullock, J.H. Jr.: Toxic substances from coal combustion—a comprehensive assessment, Phase II: element modes of occurrence for the Ohio 5/6/7, Wyodak, and North Dakota coal samples. Open-File Report 02-224, U.S. Geological Survey, U.S. Department of the Interior, p. 79 (2002)
Lackovic, K., Angove, M.J., Wells, J.D., Johnson, B.B.: Modeling the adsorption of Cd(II) onto Muloorina illite and related clay minerals. J. Colloid Interface Sci. **257**, 31–40 (2003)
Lee, F.Y., Kittirck, J.A.: Elements associated with the cadmium phase in a harbor sediment as determined with the electron beam microprobe. J. Environ. Qual. **13**(3), 337–340 (1984)
Lide, D.R. (ed.): CRC Handbook of Chemistry and Physics, 85th edn., Sect. 14, "Geophysics, Astronomy, and Acoustics; Abundance of Elements in the Earth's Crust and in the Sea". CRC Press, Boca Raton, FL (2005)
Lindberg, R.D., Runnels, D.D.: Ground water redox reactions: an analysis of equilibrium state applied to Eh measurements and geochemical modeling. Science **225**, 925–927 (1984)
Luther, G.W., Meyerson, A.L., Krajevski, J.J., Hires, R.: Metal sulfides in estuarine sediments. J. Sediment. Petrol. **50**, 1117–1120 (1980)
Lutzenkirchen, J.: Surface Complexation Modelling. pp. 638 Academic Press, Amsterdam (2006)
Manning, B.A., Goldberg, S.: Adsorption and stability of arsenic(III) at the clay mineral-water interface. Environ. Sci. Technol. **31**, 2005–2011 (1997)
McGrath, A.E., Upson, G.L., Caldwell, M.D.: Evaluation and mitigation of landfill gas impacts on cadmium leaching from native soils. Ground Water Monit. Remediat. **27**, 99–109 (2007)
Mehra, M.C., Gubeli, A.O.: Complexing characteristics of insoluble selenides. III. Mercuric selenide. J. Less-Common Metals **25**(3), 221–224 (1971)
Muller, B., Sigg, L.: Adsorption of lead(ll) on the goethite surface: voltammetric evaluation of surface complexation parameters. J. Colloid Interface Sci. **148**(2), 517–532 (1991)
Palandri, J., Kharaka, Y.K.: A compilation of rate parameters of water-mineral interaction kinetics for application to geochemical modeling. U.S. Geological Survey Open File Report 2004-1068 (2004)
Paquette, K.E., Helz, G.: Inorganic speciation of mercury in sulfidic waters: the importance of zero-valent sulfur. Environ. Sci. Technol. **31**, 2148–2153 (1997)
Plummer, L., Busby, J., Lee, R., Hanshaw, B.: Geochemical modeling of the Madison Aquifer in parts of Montana, Wyoming, and South Dakota. Water Resour. Res. **26**(9), 1981–2014 (1990)
Pruess, K., Oldenburg, C., Moridis, G.: TOUGH2 User's Guide, Version 2.0. LBNL-43134. Lawrence Berkeley National Laboratory, Berkeley, CA (1999)
Reich, M., Becker, U.: First-principles calculations of the thermodynamic mixing properties of arsenic incorporation into pyrite and marcasite. Chem. Geol. **225**, 278–290 (2006)
Rickard, D.: The solubility of FeS. Geochim. Cosmochim. Acta **70**, 5779–5789 (2006)
Robie, R.A., Hemingway, B.S.: Thermodynamic properties of minerals and related substances at 298.15 K and 1 bar (10^5 Pascals) pressure and at higher temperatures. U.S. Geol. Surv. Bull. **2131**, 461 (1995)
Rozan, T.F., Luther, G.W. III, Ridge, D., Robinson, S.: Determination of Pb complexation in oxic and sulfidic waters using pseudovoltammetry. Environ. Sci. Technol. **37**, 3845–3852 (2003)
Sato, M.: Persistency-field Eh-pH diagrams for sulfides and their application to supergene oxidation and enrichment of sulfide ore bodies. Geochim. Cosmochim. Acta **56**(8), 3133–3156 (1992)

Shaw, D.M., Dostal, J., Keays, R.R.: Additional estimates of continental surface Precambrian shield composition in Canada. Geochim. Cosmochim. Acta **40**, 73–83 (1985)
Skyllberg, U.: Competition among thiols and inorganic sulfides and polysulfides for Hg and MeHg in wetland soils and sediments under suboxic conditions: illumination of controversies and implications for MeHg net production. J. Geophys. Res. **113**, 14 (2008)
Smedley, P.L., Kinniburgh, D.G.: A review of the source, behaviour and distribution of arsenic in natural waters. Appl. Geochem. **17**, 517–568 (2002)
Smyth, R.C., Hovorka, S.D., Lu, J., Romanak, K.D., Partin, J.W., Wong, C.: Assessing risk to fresh water resources from long term CO_2 injection—laboratory and field studies. Proceedings 9th International Conference on Greenhouse Gas Control Technologies, November 2008, Washington, DC (2008)
Steefel, C.I., Lasaga, A.C.: A coupled model for transport of multiple chemical species and kinetic precipitation/dissolution reactions with applications to reactive flow in a single-phase hydrothermal system. Am. J. Sci. **294**, 529–592 (1994)
Stefansson, A., Arnorsson, S., Sveinbjornsdottir, A.E.: Redox reactions and potentials in natural waters at disequilibrium. Chem. Geol. **221**, 289–311 (2005)
Taylor, S.R., McLennan, S.M.: The Continental Crust: Its Composition and Evolution. pp. 330 Blackwell, Oxford (1985)
U.S. Environmental Protection Agency: 2004 edition of the drinking water standards and health advisories. EPA 822-R-04-005, January (2004)
USGS: Mercury in U.S. Coal—Abundance, Distribution, and Modes of Occurrence. U.S. Geological Survey Fact Sheet FS-095-01, p. 6 (2001)
Wang, S., Jaffe, P.R.: Dissolution of a mineral phase in potable aquifers due to CO_2 releases from deep formations: effect of dissolution kinetics. Energy Convers. Manag. **45**, 2833–2848 (2004)
Wänke, H., Dreibus, G., Jagoutz, E.: Mantle chemistry and accretion history of the Earth. In: Kröner, A., Hanson, A.M., Goodwin, G.N. (eds.) Archean Geochemistry, pp. 1–24. Springer, Berlin (1984)
Washington, J.W., Endale, D.M., Samarkina, L.P., Chappell, K.E.: Kinetic control of oxidation state at thermodynamically buffered potentials in subsurface waters. Geochim. Cosmochim. Acta **68**(23), 4831–4842 (2004)
Weaver, B.L., Tamey, J.: Major and trace element composition of the continental lithosphere. In: Pollack, H.N., Murthy, V.R. (eds.) Physics and Chemistry of the Earth, vol. 15, pp. 39–68. Pergamon, Oxford (1984)
Wolery, T.J.: EQ3/6, A software package for geochemical modelling of aqueous systems (Version 7.2). Lawrence Livermore Nat. Lab. UCRL-MA 110662 (1993)
Xu, T., Sonnenthal, E., Spycher, N., Pruess, K.: TOUGHREACT: a simulation program for non-isothermal multiphase reactive geochemical transport in variably saturated geologic media. Comput. Geosci. **32**, 145–165 (2006)
Xu, T., Apps, J.A., Pruess, K., Yamamoto, H.: Numerical modeling of injection and mineral trapping of CO_2 with H_2S and SO_2 in a sandstone formation. Chem. Geol. **242**, 319–346 (2007)
Zaggia, L., Zonta, R.: Metal-sulfide formation in the contaminated anoxic sludge of the Venice canals. Appl. Geochem. **12**, 527–536 (1997)
Zhang, S., Li, J., Wang, Y., Hu, G.: Dissolution kinetics of galena in acid NaCl solutions at 25–75°C. Appl. Geochem. **19**, 835–841 (2003)
Zheng, L., Apps, J.J., Spycher, N., Birkholzer, J.T., Kharaka, Y., Thorsden, J., Kakourus, E., Trautz, R.: Geochemical modeling of changes in shallow groudwater chemistry observed in the ZERT CO_2 injection experiment. In: Proceedings TOUGH2 Symposium 2009, Berkeley, CA. USA, (2009)